

RECEIVED: January 9, 2017

ACCEPTED: February 19, 2017

PUBLISHED: March 10, 2017

Search for dark matter and unparticles in events with a Z boson and missing transverse momentum in proton-proton collisions at $\sqrt{s} = 13 \text{ TeV}$



The CMS collaboration

E-mail: cms-publication-committee-chair@cern.ch

ABSTRACT: A search for dark matter and unparticle production at the LHC has been performed using events containing two charged leptons (electrons or muons), consistent with the decay of a Z boson, and large missing transverse momentum. This study is based on data collected with the CMS detector in 2015, corresponding to an integrated luminosity of 2.3 fb^{-1} of proton-proton collisions at the LHC, at a center-of-mass energy of 13 TeV. No excess over the standard model expectation is observed. Compared to previous searches in this topology, which exclusively relied on effective field theories, the results are interpreted in terms of a simplified model of dark matter production for both vector and axial vector couplings between a mediator and dark matter particles. The first study of this class of models using CMS data at $\sqrt{s} = 13 \text{ TeV}$ is presented. Additionally, effective field theories of dark matter and unparticle production are used to interpret the data.

KEYWORDS: Beyond Standard Model, Hadron-Hadron scattering (experiments)

ARXIV EPRINT: [1701.02042](https://arxiv.org/abs/1701.02042)

Contents

1	Introduction	1
2	The CMS detector	4
3	Simulation	4
4	Event reconstruction	6
5	Event selection	8
6	Background estimation	8
7	Efficiencies and systematic uncertainties	11
8	Results	13
8.1	The DM interpretation	13
8.2	Unparticle interpretation	15
8.3	Model-independent limits	15
9	Summary	16
	The CMS collaboration	26

1 Introduction

According to the well-established Λ $_{\mathrm{CDM}}$ model of cosmology, known matter only comprises about 5% of the total energy content of the universe, with 27% contributed by dark matter (DM) and the rest being dark energy [1]. Although strong astrophysical evidence indicates the existence of DM, there is no evidence yet for nongravitational interactions between DM and standard model (SM) particles. DM searches exploit a number of methods including direct detection [2] and indirect detection [3]. If there are DM particles that can be observed in direct detection experiments, they could have substantial couplings to nucleons, and therefore could be produced at the CERN LHC. A theoretically promising possibility is that DM may take the form of weakly interacting massive particles. Searches for production of such particles at colliders typically consider the case of DM recoiling against a standard model particle (“tag”) to obtain a defined signature [4]. Such searches have been performed using various standard model signatures as tags [5–20]. In models where DM production is mediated by an interaction involving SM quarks, the monojet signature is typically the most sensitive. If DM particles are instead produced via radiation emitted by a standard model boson, searches in the $Z/W/\gamma + E_T^{\mathrm{miss}}$ channels are advantageous.

The study presented here considers the case of a Z boson recoiling against a pair of DM particles, $\chi\bar{\chi}$. The Z boson subsequently decays into two charged leptons ($\ell^+\ell^-$, where $\ell = e$ or μ) producing a well-defined signature together with missing transverse momentum due to the undetected DM particles. A simplified tree-level ultraviolet-complete model [4] that contains a massive spin-1 mediator exchanged in the s -channel is considered here. In this model, the spin-1 mediator \mathcal{A} could have either vector or axial-vector couplings to the SM and DM particles. The DM particle χ is assumed to be a Dirac fermion. The interaction Lagrangian of the s -channel vector mediated DM model can be written as:

$$\mathcal{L}_{\text{vector}} = - \sum_q g_q \mathcal{A}_\mu \bar{q} \gamma^\mu q - g_\chi \mathcal{A}_\mu \bar{\chi} \gamma^\mu \chi,$$

where the mediator is labeled as \mathcal{A} , and its coupling to DM particles is labeled as g_χ . The coupling between the mediator and SM quarks is labeled as g_q , and is assumed to be universal to all quarks. The Lagrangian for an axial-vector mediator is obtained by making the replacement $\gamma^\mu \rightarrow \gamma^\mu \gamma^5$ in all terms.

As a benchmark model for DM production via a scalar coupling, an effective field theory (EFT) with dimension-7 operators is also considered [4]. It contains $SU(2)_L \times U(1)_Y$ gauge invariant couplings between a DM pair and two SM gauge bosons in a four-particle contact interaction. The corresponding interaction Lagrangian is:

$$\mathcal{L}_{\text{dim. 7}} = \frac{1}{\Lambda^3} \bar{\chi} \chi (c_1 B_{\mu\nu} B^{\mu\nu} + F_{\mu\nu}^i F^{i,\mu\nu}),$$

in which $B_{\mu\nu}$ and $F_{\mu\nu}^i$ are the $U(1)_Y$ and $SU(2)_L$ field tensors, and Λ denotes the cutoff scale. The coupling parameter c_1 controls the relative importance of the $U(1)_Y$ and $SU(2)_L$ fields for DM production. Any multiplicative factor for the $U(1)_Y$ and $SU(2)_L$ couplings is absorbed into Λ . Note that the choice of Λ modifies the signal cross section, but not the expected kinematic properties of events. The model is nonrenormalizable and should be considered as a benchmark of the sensitivity to this class of interaction. It should be used with caution when making comparisons with other sources of DM constraints, such as direct detection experiments.

Figure 1 shows the Feynman diagrams for production of DM pairs ($\chi\bar{\chi}$) in association with a Z boson in these two types of models.

The signature for DM production considered in this paper is the production of a pair of leptons (e^+e^- or $\mu^+\mu^-$) consistent with a Z boson decay, together with a large missing transverse momentum. This same signature is sensitive to other models of physics beyond the SM (BSM), e.g. “unparticles” (U).

The unparticle physics concept [21–24] is particularly interesting because it is based on scale invariance, which is anticipated in many BSM physics scenarios [25–27]. The effects of the scale invariant sector (unparticles) appear as a noninteger number of invisible massless particles. In this scenario, the SM is extended by introducing a scale invariant Banks-Zaks (BZ) field, which has a nontrivial infrared fixed point [28]. This field can interact with SM particles by exchanging heavy particles with a high mass scale M_U . Below this mass scale, the coupling is nonrenormalizable and the interaction is suppressed by powers of M_U . The

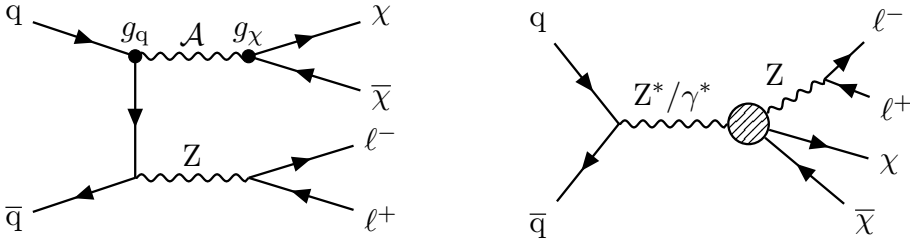


Figure 1. Leading order Feynman diagrams for production of DM pairs ($\chi\bar{\chi}$) in association with a Z boson. Left: the simplified model containing a spin-1 mediator \mathcal{A} . The constant g_q (g_χ) is the coupling strength between \mathcal{A} and quarks (DM). Right: an EFT benchmark with a DM pair coupling to gauge bosons via dimension-7 operators.

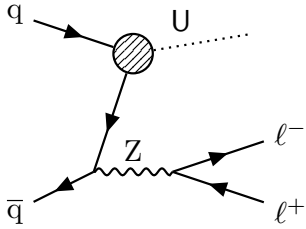


Figure 2. Leading order Feynman diagram for unparticle (denoted by U) production in association with a Z boson. The hatched circle indicates the interaction modeled with an EFT operator.

EFT Lagrangian can be expressed as:

$$\mathcal{L}_U = C_U \frac{\Lambda_U^{d_{BZ}-d_U}}{M_U^k} \mathcal{O}_{SM} \mathcal{O}_U = \frac{\lambda}{\Lambda_U^{d_U}} \mathcal{O}_{SM} \mathcal{O}_U,$$

in which C_U is a normalization factor, d_U represents the possible noninteger scaling dimension of the unparticle operator \mathcal{O}_U , \mathcal{O}_{SM} is an operator composed of SM fields with dimension d_{SM} , $k = d_{SM} + d_{BZ} - 4 > 0$ is the scaling dimension, Λ_U is the energy scale of the interaction, and d_{BZ} denotes the scaling dimension of the BZ operator at energy scales above Λ_U . The parameter $\lambda = C_U \Lambda_U^{d_{BZ}} / M_U^k$ is a measure of the coupling between SM particles and unparticles. The scaling dimension $d_U \geq 1$ is constrained by the unitarity condition. Additional details regarding this unparticle model are available in ref. [17].

In this paper, real emission of scalar unparticles is considered. The unparticles are assumed to couple to the standard model quarks in an effective three-particle interaction. In the scalar unparticle case, $\mathcal{O}_{SM} = \bar{q}q$, which yields numerically identical results to the pseudo-scalar operator choice $\mathcal{O}_{SM} = \bar{q}i\gamma_5 q$ [29]. Figure 2 shows the corresponding tree-level diagram for the production of unparticles associated with a Z boson.

The analysis is based on a data set recorded with the CMS detector in 2015 in pp collisions at a center-of-mass energy of 13 TeV, corresponding to an integrated luminosity of $2.3 \pm 0.1 \text{ fb}^{-1}$. A previous CMS search in the same final state [17], based on data collected at a center-of-mass energy of 8 TeV, found no evidence of new physics and set limits on DM and unparticle production using an EFT description. A CMS analysis of the 8 TeV data set in the combined monojet and hadronic mono-V (where V = W or Z)

channels [19] has previously set limits on the simplified model parameters considered here. Dark matter particle masses of up to 500 GeV (400 GeV) and mediator masses of up to 1.6 TeV have been excluded in the vector (axial-vector) coupling scenarios for $g_q = g_{\text{DM}} = 1$. A search performed by the ATLAS Collaboration using $\sqrt{s} = 13$ TeV data corresponding to an integrated luminosity of 3.2 fb^{-1} in events with a hadronically decaying V boson and E_T^{miss} has recently reported exclusion of the dimension-7 EFT scenario up to $\Lambda = 700$ GeV (460 GeV) for DM particle masses of 1 GeV (1 TeV) [20].

2 The CMS detector

The central feature of the CMS apparatus is a superconducting solenoid of 6 m internal diameter, providing a magnetic field of 3.8 T. Within the solenoid volume are a silicon pixel and strip tracker, a lead tungstate crystal electromagnetic calorimeter (ECAL), and a brass and scintillator hadron calorimeter (HCAL), each composed of a barrel and two endcap sections. Forward calorimeters extend the pseudorapidity (η) [30] coverage provided by the barrel and endcap detectors. Muons are measured in gas-ionization detectors embedded in the steel flux-return yoke outside the solenoid. A more detailed description of the CMS detector, together with a definition of the coordinate system used and the relevant kinematic variables, can be found in ref. [30].

Variables of particular relevance to the present analysis are the missing transverse momentum vector \vec{p}_T^{miss} and the magnitude of this quantity, E_T^{miss} . The quantity \vec{p}_T^{miss} is defined as the projection on the plane perpendicular to the beams of the negative vector sum of the momenta of all reconstructed particles in an event.

3 Simulation

Samples of simulated DM particle events for both the simplified model and EFT interpretations are generated using MADGRAPH5_aMC@NLO 2.2.2 [31] at leading order (LO) and matched to PYTHIA 8.205 [32] using tune CUETP8M1 for parton showering and hadronization [33, 34]. The factorization and renormalization scales are set to the geometric mean of $\sqrt{p_T^2 + m^2}$ for all final-state particles [4, 31], where p_T and m are the transverse momentum and mass of each particle.

For the simplified model of DM production, couplings are chosen according to the recommendations in ref. [35]. The coupling g_χ is set to unity. For g_q , values of 1.0 and 0.25 are considered. The width of the mediator is assumed to be determined exclusively by the contributions from the couplings to quarks and the DM particle χ . Under this assumption, the width is in the range 1–5% (30–50%) of the mediator mass for $g_q = 0.25$ ($g_q = 1.00$). The signal simulation samples with $g_q = 1.0$ are processed using the detector simulation described below. Signal predictions for $g_q = 0.25$ are obtained by applying event weights based on the E_T^{miss} distribution at the generator level to the fully simulated samples with $g_q = 1.0$. This procedure allows to take into account any effect of the coupling dependent mediator width on the E_T^{miss} distribution [35]. The exact dependence of the width on the model parameters is reported in [35].

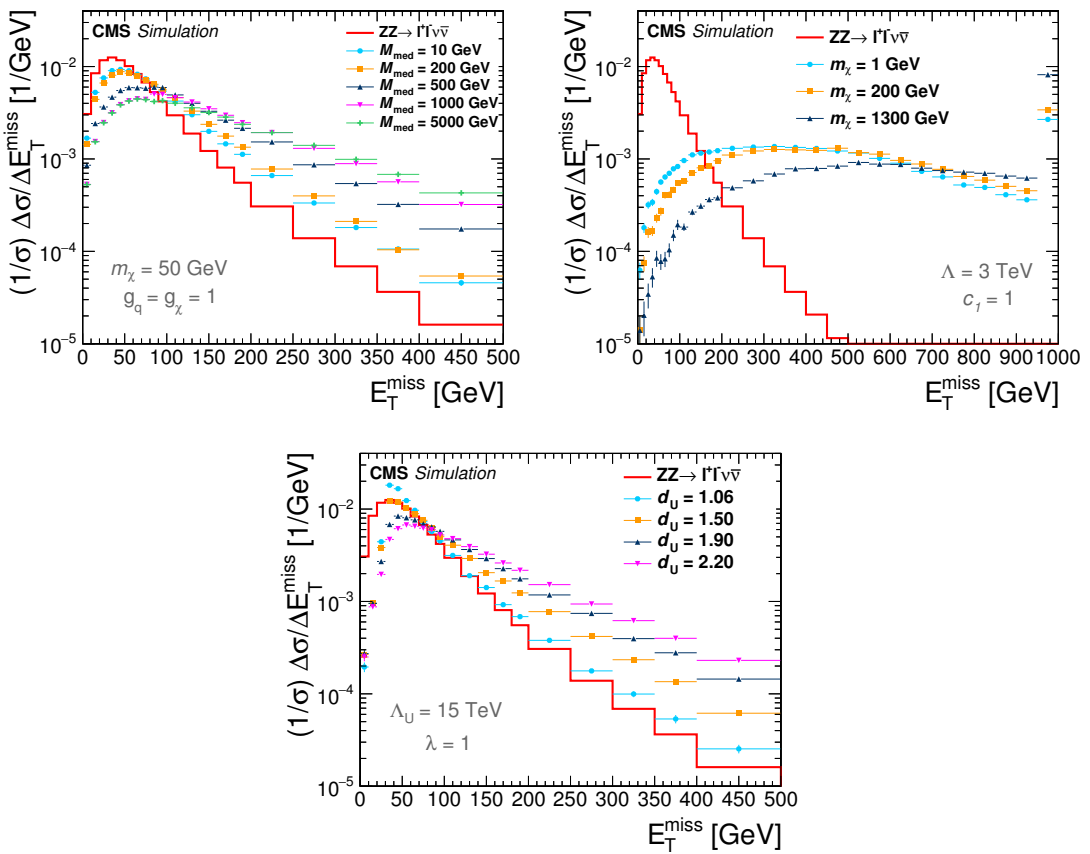


Figure 3. The distribution in E_T^{miss} at the generator level, for the simplified DM model with vector mediator (upper left), EFT DM model (upper right), and unparticle scenarios (lower panel). The y-axis corresponds to the integrated cross section per bin divided by the total cross section and bin width. The DM curves are shown for different values of the vector mediator mass M_{med} in the upper left panel and for different values of the DM mass m_χ in the upper right panel. The unparticle curves have the scalar unparticle coupling λ between unparticle and SM fields set to 1. They are shown for several values of the scaling dimension d_U ranging from 1.06 to 2.20, spanning the region of sensitivity of this analysis. The SM background $ZZ \rightarrow \ell^-\ell^+\nu\bar{\nu}$ is shown as a red solid histogram. The rightmost bins include overflow.

Samples for the EFT DM benchmark are generated with $\Lambda = 3 \text{ TeV}$ and $c_1 = 1$. Signal predictions for other values of Λ are obtained by rescaling the signal cross section accordingly, while other values of c_1 are evaluated using the same reweighting method as for the simplified model case.

The events for the unparticle model are generated at LO with PYTHIA 8 [29, 36] assuming a cutoff scale $\Lambda_U = 15 \text{ TeV}$, using tune CUETP8M1 for parton showering and hadronization. We evaluate other values of Λ_U by rescaling the cross sections as needed. The parameter Λ_U acts solely as a scaling factor for the cross section and does not influence the kinematic distributions of unparticle production [29].

The POWHEG 2.0 [37–41] event generator is used to produce samples of events for the $t\bar{t}$, tW , $q\bar{q} \rightarrow ZZ$, and WZ background processes, which are simulated at next-to-leading

order (NLO). The $gg \rightarrow ZZ$ process is simulated using MCFM 7.0.1 [42] at NLO. The Drell-Yan ($DY, Z/\gamma^* \rightarrow \ell^+\ell^-$) process is generated using the MADGRAPH5_aMC@NLO event generator at LO and normalized to the next-to-next-to-leading order (NNLO) cross section as calculated using FEWZ 3.1 [43, 44]. Triboson events (WZZ, WWZ and ZZZ) are simulated using MADGRAPH5_aMC@NLO at NLO. Samples of quantum chromodynamics (QCD) production of multijet events are generated using PYTHIA 8 at LO. For all SM simulation samples, parton showering and hadronization are performed with PYTHIA 8 with tune CUETP8M1.

The parton distribution function (PDF) set NNPDF3.0 [45] is used for Monte Carlo (MC) samples, and the detector response is simulated using a detailed description of the CMS detector, based on the GEANT4 package [46, 47]. Minimum bias events are superimposed on the simulated events to emulate the effect of additional pp interactions in the same or nearby bunch crossings (pileup). All MC samples are corrected to reproduce the pileup distribution as measured in the data. The average number of pileup interactions per proton bunch crossing is about 12 for the 2015 data sample.

The upper left panel of figure 3 shows the distribution of E_T^{miss} at the generator level for DM particles with a mass of 50 GeV in the simplified model. The events generated with larger mediator mass M_{med} tend to have a broader E_T^{miss} distribution and reach further into the high- E_T^{miss} regime. The analogous distributions in the EFT benchmark model with DM masses $m_\chi = 1, 200$, and 1300 GeV are shown in the upper right panel of figure 3. In the unparticle scenario, the events generated with larger scaling dimension d_U tend to preferentially populate the high- E_T^{miss} regime, as shown in the lower panel of figure 3. The SM background $ZZ \rightarrow \ell^-\ell^+\nu\bar{\nu}$ is shown in all plots for comparison, as a red solid histogram.

4 Event reconstruction

Events are collected by requiring dilepton triggers (ee or $\mu\mu$) with a threshold of $p_T > 17$ GeV for the leading lepton. The threshold for the subleading lepton is $p_T > 12$ (8) GeV for electrons (muons). Single-lepton triggers with thresholds of $p_T > 23$ (20) GeV for electrons (muons) are also included to recover residual trigger inefficiencies. Prior to the selection of leptons, the primary vertex [48] with the largest value of $\sum p_T^2$ for the associated tracks is selected as the event vertex. Simulation studies show that this requirement correctly selects the event vertex in more than 99% of both signal and background events. The lepton candidate tracks are required to be compatible with the event vertex.

A particle-flow (PF) event algorithm [49, 50] reconstructs and identifies each individual particle with an optimized combination of information from the various elements of the CMS detector. Photon energies are directly obtained from the ECAL measurement, corrected for zero-suppression effects [30]. Electron energies are determined from a combination of the electron momentum at the event vertex as determined by the tracker, the energy of the corresponding ECAL cluster, and the energy sum of all bremsstrahlung photons spatially compatible with originating from the electron track. Muon momenta are obtained from the curvature of the corresponding track. Charged hadron energies are determined from a combination of their momentum measured in the tracker and the

matching ECAL and HCAL energy deposits, corrected for zero-suppression effects and for the response function of the calorimeters to hadronic showers [50]. Finally, neutral hadron energies are obtained from the corresponding corrected ECAL and HCAL energies.

Electron candidates are reconstructed using an algorithm that combines information from the ECAL and the tracker [51]. To reduce the electron misidentification rate, the candidates have to satisfy additional identification criteria that are based on the shape of the electromagnetic shower in the ECAL. In addition, the electron track is required to originate from the event vertex and to match the shower cluster in the ECAL. Electron candidates with an ECAL cluster in the transition region between ECAL barrel and endcap ($1.44 < |\eta| < 1.57$) are rejected because the reconstruction of an electron candidate in this region is not optimal. Candidates that are identified as coming from photon conversions [51] in the detector material are explicitly removed.

Muon candidate reconstruction is based on two algorithms: in the first, tracks in the silicon tracker are matched with at least one muon segment in any detector plane of the muon system, and in the second algorithm, a combined fit is performed to hits in both the silicon tracker and the muon system [52]. The muon candidates in this analysis are required to be reconstructed with at least one of the two algorithms and to be further identified as muons by the PF algorithm. To reduce the muon misidentification rate, additional identification criteria are applied based on the number of spatial points measured in the tracker and in the muon system, the fit quality of the muon track, and its consistency with the event vertex location.

Leptons produced in the decay of Z bosons are expected to be isolated from hadronic activity in the event. Therefore, an isolation requirement is applied based on the sum of the momenta of the PF candidates found in a cone of radius $\Delta R = 0.4$ around each lepton. The isolation sum is required to be smaller than 15% (20%) of the p_T of the electron (muon). For each electron, the mean energy deposit in the isolation cone of the electron, coming from other pp collisions in the same bunch crossing, is estimated following the method described in ref. [51], and subtracted from the isolation sum. For muon candidates, only charged tracks associated with the event vertex are included. The sum of the p_T for charged particles not associated with the event vertex in the cone of interest is rescaled by a factor of 0.5, corresponding to the average neutral to charged energy density ratio in jets, and subtracted from the isolation sum.

For the purpose of rejecting events containing τ leptons, hadronically decaying τ leptons (τ_h) are identified using the “hadron-plus-strips” algorithm. The algorithm identifies a jet as a τ_h candidate if a subset of the particles assigned to the jet is consistent with the decay products of a τ_h [53]. In addition, τ_h candidates are required to be isolated from other activity in the event.

Jets are reconstructed from PF candidates by using the anti- k_T clustering algorithm [54] with a distance parameter of 0.4, as implemented in the FASTJET package [55, 56]. Jets are identified over the full calorimeter acceptance, $|\eta| < 5$. The jet momentum is defined as the vector sum of all particle momenta assigned to the jet, and is found in simulation to be within 5 to 10% of the true hadron-level momentum over the whole p_T range and detector acceptance. An overall energy subtraction is applied to correct for the extra energy clustered in jets due to pileup, following the procedure described

in ref. [57]. Additional corrections to the jet energy scale and resolution are derived from simulation, and are complemented by measurements of the energy balance in dijet and γ +jets events [57].

5 Event selection

A preselection with a large yield is used to validate the background model and is followed by a final selection that is designed to give maximal sensitivity to the signal, as quantified by the expected limits achieved. Preselected events are required to have exactly two well-identified, isolated leptons with the same flavor and opposite charge (e^+e^- or $\mu^+\mu^-$), each with $p_T > 20\text{ GeV}$. The invariant mass of the lepton pair is required to be within $\pm 10\text{ GeV}$ of the nominal mass of the Z boson [58]. Only electrons (muons) within the range of $|\eta| < 2.5$ (2.4) are considered. To reduce the background from the WZ process where the W boson decays leptonically, events are removed if an additional electron or muon is reconstructed with $p_T > 10\text{ GeV}$. The event is also removed from the final selection if a τ_h candidate is reconstructed with $p_T > 20\text{ GeV}$. As a loose preselection requirement, the dilepton transverse momentum ($p_T^{\ell\ell}$) is required to be larger than 50 GeV to reject the bulk of DY background events.

Since only a small amount of hadronic activity is expected in the final state of both DM and unparticle events, any event having two or more jets with $p_T > 30\text{ GeV}$ is rejected. Processes involving top quarks are further suppressed with the use of techniques based on soft-muon and secondary-vertex b jet tagging, aimed at identifying the b quarks produced in top quark decays. Soft muons are identified using a specialised low- p_T set of identification criteria focused on the muon candidate track quality. The rejection of events with soft muons having $p_T > 3\text{ GeV}$ reduces the background from semileptonic decays of B mesons. The b jet tagging technique employed is based on the “combined secondary vertex” algorithm [59, 60]. The algorithm is calibrated to provide, on average, 80% efficiency for tagging jets originating from b quarks, and 10% probability of light-flavor jet misidentification. Events are rejected if at least one b-tagged jet is reconstructed with $p_T > 20\text{ GeV}$ within the tracker acceptance ($|\eta| < 2.5$).

For the final selection, further kinematic requirements are set in order to achieve the best possible signal extraction. A minimal E_T^{miss} of 80 GeV is required. The angle between the Z boson and the missing transverse momentum in the transverse plane $\Delta\phi_{\ell\ell,\vec{p}_T^{\text{miss}}}$ is required to be larger than 2.7 radians. The momentum balance of the event defined by $|E_T^{\text{miss}} - p_T^{\ell\ell}|/p_T^{\ell\ell}$ is required to be smaller than 0.2 . These variables suppress background processes such as DY and top quark production. The event selection criteria used for the electron and muon channels are the same. They are summarized in table 1.

Figure 4 shows the distributions of E_T^{miss} after preselection in the ee and $\mu\mu$ channels.

6 Background estimation

The ZZ and WZ backgrounds are modeled using MC simulation, and normalized to their respective NLO cross sections. Other backgrounds, including $t\bar{t}$, tW, WW, $Z \rightarrow \tau\tau$, single top quark, and DY production are estimated from data for the final selection.

	Variable	Requirements
Preselection	p_T^ℓ	$>20 \text{ GeV}$
	$ m_{\ell\ell} - m_Z $	$<10 \text{ GeV}$
	Jet counting	$\leq 1 \text{ jet with } p_T^j > 30 \text{ GeV}$
	$p_T^{\ell\ell}$	$>50 \text{ GeV}$
	3 rd -lepton veto	$p_T^{e,\mu} > 10 \text{ GeV}, p_T^\tau > 20 \text{ GeV}$
Selection	Top quark veto	Veto on b jets and soft muons
	$\Delta\phi_{\ell\ell, p_T^{\text{miss}}}$	$>2.7 \text{ radians}$
	$ E_T^{\text{miss}} - p_T^{\ell\ell} /p_T^{\ell\ell}$	<0.2
	E_T^{miss}	$>80 \text{ GeV}$

Table 1. Summary of selections used in the analysis.

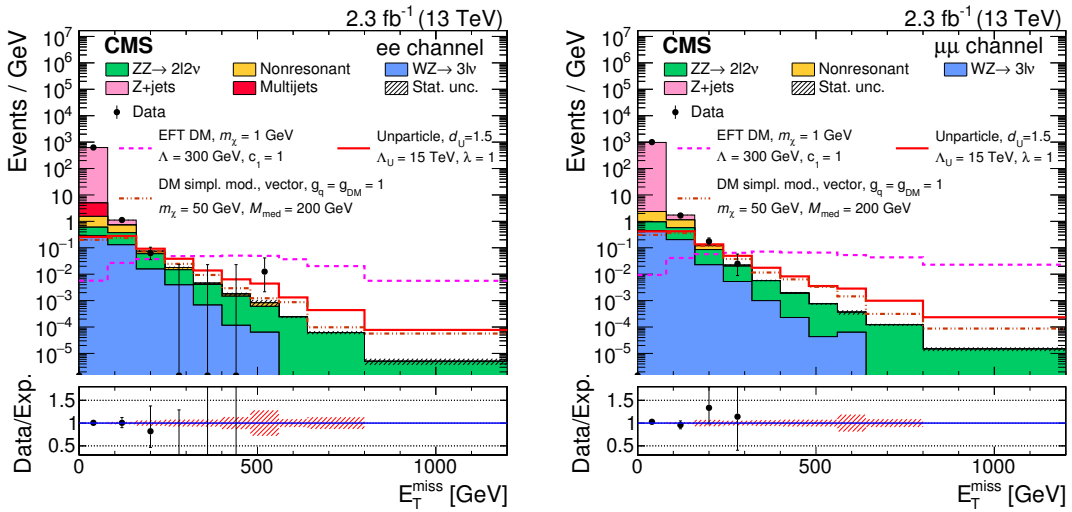


Figure 4. The distribution of E_T^{miss} after preselection for the $Z \rightarrow e^+e^-$ (left) and $Z \rightarrow \mu^+\mu^-$ (right) channels. Representative expected signal distributions are shown for the simplified model of DM production with vector couplings, the EFT scenario of DM production, and unparticles. The SM expectation is based on simulation only. The total statistical uncertainty in the overall background prediction is shown as a hatched region. Overflow events are included in the rightmost bins. The upper error bars on data points are shown for bins with zero entries (Garwood procedure) in the region up to the last non-zero entry. In the lower panels, the ratio between data and predicted background is shown.

The simulation of the ZZ process includes the $q\bar{q}$ - and gg-induced production modes. In order to correct the ZZ differential cross section from NLO to NNLO in QCD, $\Delta\phi(Z, Z)$ -dependent K -factors are applied [61]. We apply NLO electroweak (EW) K -factors as a function of the p_T of the trailing boson, following the calculations in refs. [62–64]. Electroweak corrections to WZ production are also available, but considered small [64] and not applied.

The background processes involving ee or $\mu\mu$ pairs not directly resulting from the decay of a Z boson are referred to as nonresonant backgrounds. These backgrounds arise

mainly from leptonic W boson decays in $t\bar{t}$, tW, and WW events. There are also small contributions from the s - and t -channel single top quark events, W+jets events, and $Z \rightarrow \tau\tau$ events in which τ lepton decays result in electrons or muons and E_T^{miss} . We estimate these nonresonant backgrounds using a data control sample, consisting of events with opposite-charge different-flavor dilepton pairs ($e^\pm\mu^\mp$) that otherwise pass the full selection. As the decay rates for $Z \rightarrow e^+e^-$ and $Z \rightarrow \mu^+\mu^-$ are almost equal, by equating the ratio of observed dilepton counts to the square of the ratio of efficiencies, the nonresonant backgrounds in the ee and $\mu\mu$ channels can be estimated from the $e\mu$ channel:

$$N_{\text{bkg},\text{ee}}^{\text{est}} = N_{e\mu}^{\text{data, corr}} k_{\text{ee}}, \quad k_{\text{ee}} = \frac{1}{2} \sqrt{\frac{N_{\text{ee}}^{\text{data}}}{N_{\mu\mu}^{\text{data}}}},$$

$$N_{\text{bkg},\mu\mu}^{\text{est}} = N_{e\mu}^{\text{data, corr}} k_{\mu\mu}, \quad k_{\mu\mu} = \frac{1}{2} \sqrt{\frac{N_{\mu\mu}^{\text{data}}}{N_{\text{ee}}^{\text{data}}}},$$

in which the coefficient of 1/2 in the transfer factors k_{ee} and $k_{\mu\mu}$ comes from the dilepton decay ratios for ee, $\mu\mu$, and $e\mu$ in these nonresonant backgrounds, and $N_{\text{ee}}^{\text{data}}$ and $N_{\mu\mu}^{\text{data}}$ are the numbers of selected ee and $\mu\mu$ events from data with masses in the Z boson mass window. The ratio $\sqrt{N_{\text{ee}}^{\text{data}}/N_{\mu\mu}^{\text{data}}}$ and the reciprocal quantity take into account the difference between the electron and muon selection efficiencies. The term $N_{e\mu}^{\text{data, corr}}$ is the number of $e\mu$ events observed in data corrected by subtracting the estimated ZZ, WZ, and DY background contributions. The kinematic distributions of the estimated nonresonant backgrounds are obtained from simulation with the overall normalization determined by the method described above. The validity of this procedure for predicting nonresonant backgrounds is checked with simulated events containing $t\bar{t}$, tW, WW, W+jets, and $Z \rightarrow \tau\tau$ processes. We assign a systematic uncertainty of 26% for this background estimation in both the electron and muon channels for $E_T^{\text{miss}} > 80$ GeV, based on closure tests that compare the predictions obtained from the control sample with those from the simulated events.

The DY process is dominant in the region of low E_T^{miss} . This process does not produce undetectable particles, and therefore the measured E_T^{miss} arises from limited detector acceptance and mismeasurement of particle momenta. The estimation of this background uses simulated DY events, which are normalized to data with scale factors obtained by measuring the number of DY events in a background-dominated control region, after subtracting other processes. These scale factors are of order 1.0–1.2. The control region is defined by applying the full selection with the E_T^{miss} requirement inverted. The reliability of this approach in the high- E_T^{miss} regime has been studied by considering variables sensitive to E_T^{miss} mismeasurement, such as the angular separation between the E_T^{miss} direction and any jet. A normalization uncertainty of 100%, which accommodates any differences observed in these control regions, is assigned for the DY background estimate. The assigned uncertainty has little impact on the overall signal sensitivity because of the small overall contribution from the DY background prediction.

Contributions from QCD production of multijet events is estimated using simulation and found to be negligible after final selection.

7 Efficiencies and systematic uncertainties

The efficiencies for selecting, reconstructing, and identifying isolated leptons are determined from simulation, and corrected with scale factors determined from applying a “tag-and-probe” technique [65] to $Z \rightarrow \ell^+ \ell^-$ events in data. The trigger efficiencies for the electron and muon channels are found to be above 90%, varying as a function of p_T and η of the lepton. The identification efficiency, when applying the selection criteria described in section 4, is found to be about 80–86% for electrons and 95% for muons, depending on the p_T and η of the corresponding lepton. The corresponding data-to-MC scale factors are typically in the range 0.96–1.00 for the electron and 0.96–0.98 for the muon channel, depending on the p_T and $|\eta|$ of the lepton candidate. The lepton momentum scale uncertainty is computed by varying the momentum of the leptons by its uncertainties. The lepton momentum uncertainty is 1% for the muons, while the uncertainty for the electrons is 2% in the barrel and 5% in the endcaps. For both channels, the overall uncertainty in the efficiency of selecting and reconstructing leptons in an event is about 3%.

In the treatment of systematic uncertainties, both normalization effects, which only affect the overall size of individual contributions, as well as shape uncertainties, which also affect their distribution, are taken into account. The systematic uncertainties are summarized in table 2. Where applicable, the symbol V is used to refer to both Z and W bosons. The impact of each source of uncertainty on the observed strength of a potential signal is also reported. The signal strength is defined as the ratio of the observed or excluded signal cross-section to the signal cross-section predicted by theory. To calculate the impact, a maximum likelihood fit of the combined background and signal model to the expected distribution for unity signal strength is performed. The fit is repeated with each individual nuisance parameter varied by its uncertainty. The impact of the uncertainty is then defined as the relative change induced in the expected best fit signal strength by the variation of the respective parameter. In the table, the reference signal is the simplified model DM scenario with a vector mediator of mass 200 GeV, a DM particle mass of 50 GeV, and coupling $g_q = 1.0$.

The normalization uncertainties in the background estimates from data have been described in section 6. The PDF and α_S uncertainties (referred to as PDF+ α_S in the following) for signal and background processes are estimated from the standard deviation (s.d.) of weights according to the replicas provided in the NNPDF3.0 parton distribution set [66]. While the influence on the estimated signal acceptance arising from theory-related uncertainties is included in the limit calculation, the corresponding effect on the normalization of the signal process is not. For the simplified model of DM production, the effect of the signal normalization uncertainty is treated separately from the experimental uncertainty and is shown as a dashed band around the observed limit. Since the EFT benchmark and unparticle scenarios are extremely simplified, theory-related cross-section uncertainties are not considered to be realistic for these models and are thus neglected. The efficiencies for signal, ZZ, and WZ processes are estimated using simulation, and the uncertainties in the corresponding yields are derived by varying the renormalization and factorization scales, α_S , and choice of PDFs. The factorization and renormalization scale

Source of uncertainty	Background uncertainty (%)	Signal uncertainty (%)	Impact (%)
Integrated luminosity	2.7	2.7	5
Lepton trigger & identification efficiency	3–4	3–4	2–4
Lepton momentum scale, resolution	1–7	<1	1–2
Jet energy scale, resolution	0.1–4.0	<1	2
b jet tagging efficiency	<1	<1	<1
Pileup	1–2	0.5–1.0	2
PDF, α_S	2–3	<1	<1
Factorization, renormalization scales (signal)	—	1–2	<1
Factorization, renormalization scales (VV)	3–4	—	3
Factorization, renormalization scales (VVV)	12	—	<1
EW correction for $q\bar{q} \rightarrow ZZ$	5	—	4
EW uncertainty for WZ	3	—	<1
DY normalization	100	—	5
t <bar>t>, tW, WW normalization</bar>	26	—	2–4
MC sample size (signal)	—	1.5–10.0	<1
MC sample size (ZZ, WZ)	0.3–3.0	—	<1
MC sample size (DY)	13	—	<1
MC sample size (t <bar>t>, tW, WW)</bar>	8–10	—	<1

Table 2. Summary of systematic uncertainties. Each background uncertainty represents the variation of the relative yields of the particular background components. The signal uncertainties represent the relative variations in the signal acceptance, and the ranges quoted cover both signals of DM and unparticles with different DM masses or scaling dimensions. For shape uncertainties, the numbers correspond to the overall effect of the shape variation on the yield or acceptance. The symbol “—” indicates that the systematic uncertainty is not applicable. The impact of each group of systematic uncertainties is calculated by performing a maximum likelihood fit to obtain the signal strength with each parameter separately varied by its uncertainty. The number given in the impact column is the relative change of the expected best fit signal strength that is introduced by the variation for the simplified model signal scenario with a vector mediator of mass 200 GeV, DM of mass 50 GeV, and coupling $g_q = 1.0$.

uncertainties are assessed by varying the original scales by factors of 0.5 or 2.0, and amount to 2–3% for ZZ and WZ processes. The effect of variations in α_S and choice of PDFs is 2% for the ZZ and WZ backgrounds. A 3% normalization uncertainty is assigned to the WZ background to account for higher-order EW corrections [64]. The uncertainty assigned to the integrated luminosity measurement is 2.7% [67].

Experimental sources of shape uncertainty are the lepton momentum scale, the jet energy scale and resolution, the b tagging efficiency, and the pileup modeling. The effect of each uncertainty is estimated by varying the respective variable of interest by its uncertainties, and propagating the variations to the distribution of E_T^{miss} after the final selection. In the case of the lepton momentum scale, the uncertainty is computed by varying the momentum of the leptons by their uncertainties. The uncertainty due to the lepton momentum scale is evaluated to be less than 1% (1–7%) for signal (background).

The uncertainties in the calibration of the jet energy scale and resolution directly affect the assignments of jets to jet categories, the E_T^{miss} computation, and all the selections related to jets. The effect of the jet energy scale uncertainty is estimated by varying the energy scale by ± 1 s.d. A similar strategy is used to evaluate the systematic uncertainty related to the jet energy resolution. The effect of the shifts is propagated to E_T^{miss} . The uncertainties in the final yields are found to be less than 1% for signal and less than 4% for background.

In order to reproduce b tagging efficiencies observed in data, an event-by-event reweighting using data-to-simulation scale factors is applied to simulated events. The uncertainty associated with this procedure is obtained by varying the event-by-event weight by ± 1 s.d. The total uncertainty in the final yields due to b tagging is less than 1% for both signal and background. All simulated events are reweighted to reproduce the pileup conditions observed in data. To compute the uncertainty related to pileup modeling, we shift the mean of the distribution in simulation by 5% [68]. The variation of the final yields induced by this procedure is 0.5–1% for signal and 1–2% for background. For the processes estimated from simulation, the sizes of the MC samples limit the precision of the modeling, and the resulting statistical uncertainty is incorporated into the shape uncertainty. A similar treatment is applied to the backgrounds estimated from control samples in data, based on the statistical uncertainties in the corresponding control samples.

8 Results

For both the electron and the muon channels, a shape-based analysis is employed. The expected numbers of background and signal events scaled by a signal strength modifier are combined in a binned likelihood for each bin of the E_T^{miss} distribution. The numbers of observed and expected events are shown in table 3, which also includes the expectation for a selected parameter point for each type of signal. Figure 5 shows the E_T^{miss} distributions after the final selection. The observed distributions agree with the SM background predictions and no excess of events is observed.

Upper limits on the contribution of events from new physics are computed by using the modified frequentist approach CL_s [69–71].

8.1 The DM interpretation

The results are interpreted in the context of a simplified model of DM production. Figure 6 shows 95% confidence level (CL) expected and observed limits on the signal strength $\sigma^{\text{obs}}/\sigma^{\text{th}}$ in the case of vector and axial-vector mediators and for two possible values of the quark-mediator coupling constant, $g_q = 0.25$ or 1. Independent of the type of coupling, production of DM particles via an on-shell mediator ($2m_\chi < M_{\text{med}}$) can be excluded up to mediator masses of ≈ 400 GeV for $g_q = 1.0$ and up to ≈ 300 GeV for $g_q = 0.25$. Dark matter particle masses are probed up to 100–150 GeV for vector and up to 50–100 GeV for axial-vector couplings. For $g_q = 1.0$, a small region of off-shell parameter space can also be excluded. In the case of $g_q = 0.25$, sensitivity is limited to the on-shell region.

Process	e^+e^-	$\mu^+\mu^-$
Simplified DM model, vector mediator $m_\chi = 50 \text{ GeV}$, $M_{\text{med}} = 200 \text{ GeV}$	$15.8 \pm 0.4 \pm 1.0$	$25.5 \pm 0.5 \pm 1.8$
Simplified DM model, axial-vector mediator $m_\chi = 50 \text{ GeV}$, $M_{\text{med}} = 200 \text{ GeV}$	$12.9 \pm 0.3 \pm 0.9$	$19.2 \pm 0.4 \pm 1.3$
EFT DM model $m_\chi = 1 \text{ GeV}$, $\Lambda = 300 \text{ GeV}$	$25.4 \pm 0.4 \pm 2.7$	$47.7 \pm 0.5 \pm 5.9$
Unparticle model $d_U = 1.05$, $\Lambda_U = 15 \text{ TeV}$	$21.5 \pm 0.6 \pm 0.9$	$31.0 \pm 0.7 \pm 1.6$
$Z/\gamma^* \rightarrow \ell^+\ell^-$	$4.9 \pm 0.6 \pm 4.9$	$5.3 \pm 0.7 \pm 5.3$
$WZ \rightarrow 3\ell\nu$	$4.6 \pm 0.2 \pm 0.4$	$7.0 \pm 0.2 \pm 0.6$
$ZZ \rightarrow 2\ell 2\nu$	$12.4 \pm 0.1 \pm 1.0$	$18.7 \pm 0.1 \pm 1.5$
$t\bar{t}/tW/\text{WW}/Z \rightarrow \tau\tau$	$7.0 \pm 1.0 \pm 1.9$	$14.0 \pm 2.1 \pm 3.8$
$VVV, ZZ \rightarrow 2\ell 2q, 4\ell$	<0.1	<0.1
Total background	$28.9 \pm 1.2 \pm 5.4$	$45.0 \pm 2.2 \pm 6.8$
Data	22	44

Table 3. Signal predictions and background estimates for the final selection with $E_T^{\text{miss}} > 80 \text{ GeV}$. The DM signal yields from the simplified model are given for mass $m_\chi = 50 \text{ GeV}$ and a mediator mass $M_{\text{med}} = 200 \text{ GeV}$ for both the vector and axial-vector coupling scenarios. For the EFT benchmark with DM pair coupling to gauge bosons, the signal yields are given for $m_\chi = 1 \text{ GeV}$, cutoff scale $\Lambda = 300 \text{ GeV}$, and the coupling $c_1 = 1$. Yields for the unparticle model are shown for scaling dimension $d_U = 1.05$, and cutoff scale $\Lambda = 15 \text{ TeV}$. The corresponding statistical and systematic uncertainties are shown, in that order.

The simplified model allows a calculation of the DM relic abundance in the universe for each parameter point [72, 73]. Parameter combinations consistent with measurements of the DM relic abundance in the universe are indicated in figure 6. For these parameter combinations, no BSM phenomena other than the simplified model are needed to account for the relic abundance in the universe. For other parameter values, additional phenomena, such as an extended dark sector, are necessary.

The exclusion limits in the $M_{\text{med}}-m_\chi$ plane are translated into limits on the DM-nucleon scattering cross section using the prescription of ref. [35]. The limits are set at 90% CL, assuming $g_q = 0.25$. The resulting exclusion curves for both spin-independent (vector) and spin-dependent (axial-vector) cases are shown in figure 7, which compares them to the results from direct detection experiments. The comparison of collider and direct detection experiments highlights the complementarity of the two approaches. Especially in the case of lower DM masses and axial-vector couplings, a collider-based search can exclude parameter space not covered by direct detection experiments. In all cases, the DM-mediator coupling g_χ is set to one.

Figure 8 shows 95% CL expected limits on the cutoff scale Λ of the EFT benchmark model with DM pair coupling to gauge bosons. The limits are derived as a function of

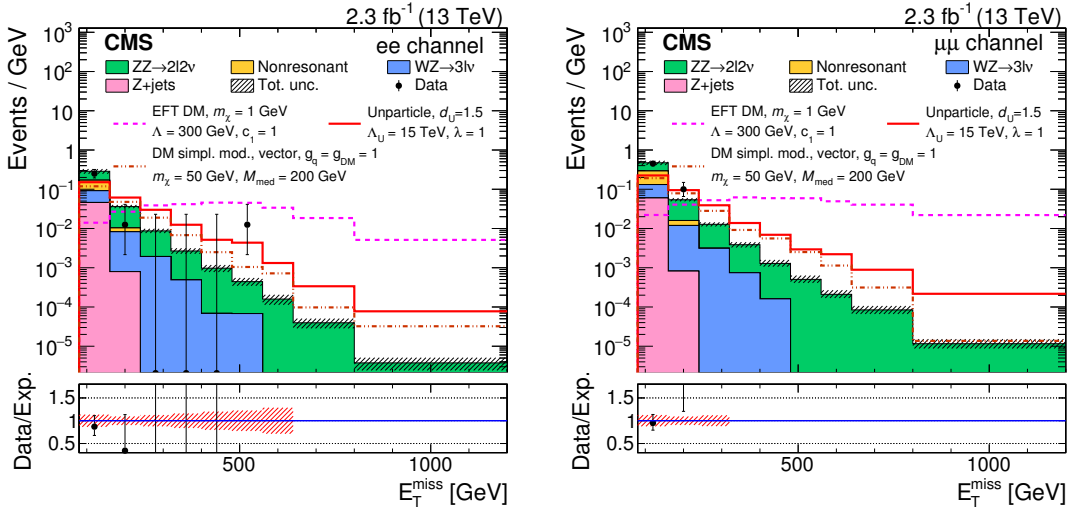


Figure 5. Distributions of E_T^{miss} for the final selection in the e^+e^- (left) and $\mu^+\mu^-$ (right) channels. Expected signal distributions are shown for the simplified model of DM production with vector couplings, the EFT DM production benchmark, and unparticle model. The total uncertainty (stat. \oplus sys.) in the overall background is shown as a hatched region. Overflow events are included in the rightmost bins. In the lower panels, the ratio between data and predicted background is shown.

the DM particle mass. At low masses, cutoff scales up to $\approx 480 \text{ GeV}$ can be excluded. With increasing DM particle mass, sensitivity decreases with $\Lambda < 250 \text{ GeV}$ excluded for $m_\chi = 1.3 \text{ TeV}$. The 95% CL expected limits on the cutoff scale Λ and signal strength $\sigma^{\text{obs}}/\sigma^{\text{th}}$ as a function of coupling c_1 and DM mass m_χ are shown in figure 9. At $c_1 \approx 1$, the interaction is dominated by the $ZZ\chi\chi$ -vertex. With increasing c_1 , the $\gamma Z\chi\chi$ -vertex begins to contribute, yielding an improvement in the sensitivity.

8.2 Unparticle interpretation

In the unparticle scenario, 95% CL lower limits are set on the effective cutoff scale Λ_U . A fixed coupling $\lambda = 1$ is assumed. The limits on Λ_U are shown in figure 10 as a function of the scaling dimension d_U . The result is compared with the limits obtained from previous CMS searches in the monojet [15] and mono-Z [17] channels, as well as with a reinterpretation of LEP searches [83]. Comparable sensitivity to the previous CMS mono-Z search is achieved owing to the increase in collision energy, which offsets the larger size of the previous dataset.

8.3 Model-independent limits

As an alternative to the interpretation of the results in specific models, a simple counting experiment is performed to obtain model-independent expected and observed 95% CL upper limits on the visible cross section $\sigma_{\text{vis}}^{\text{BSM}} = \sigma A \epsilon$ for BSM physics processes, where A is the acceptance and ϵ is the identification efficiency for a hypothetical signal. The limits as a function of E_T^{miss} thresholds are shown in figure 11. Table 4 shows the total SM background predictions for the numbers of events passing the selection requirements, for different E_T^{miss} thresholds, compared with the observed numbers of events. The 95% CL expected and observed upper limits for the contribution of events from BSM sources are also shown. Since

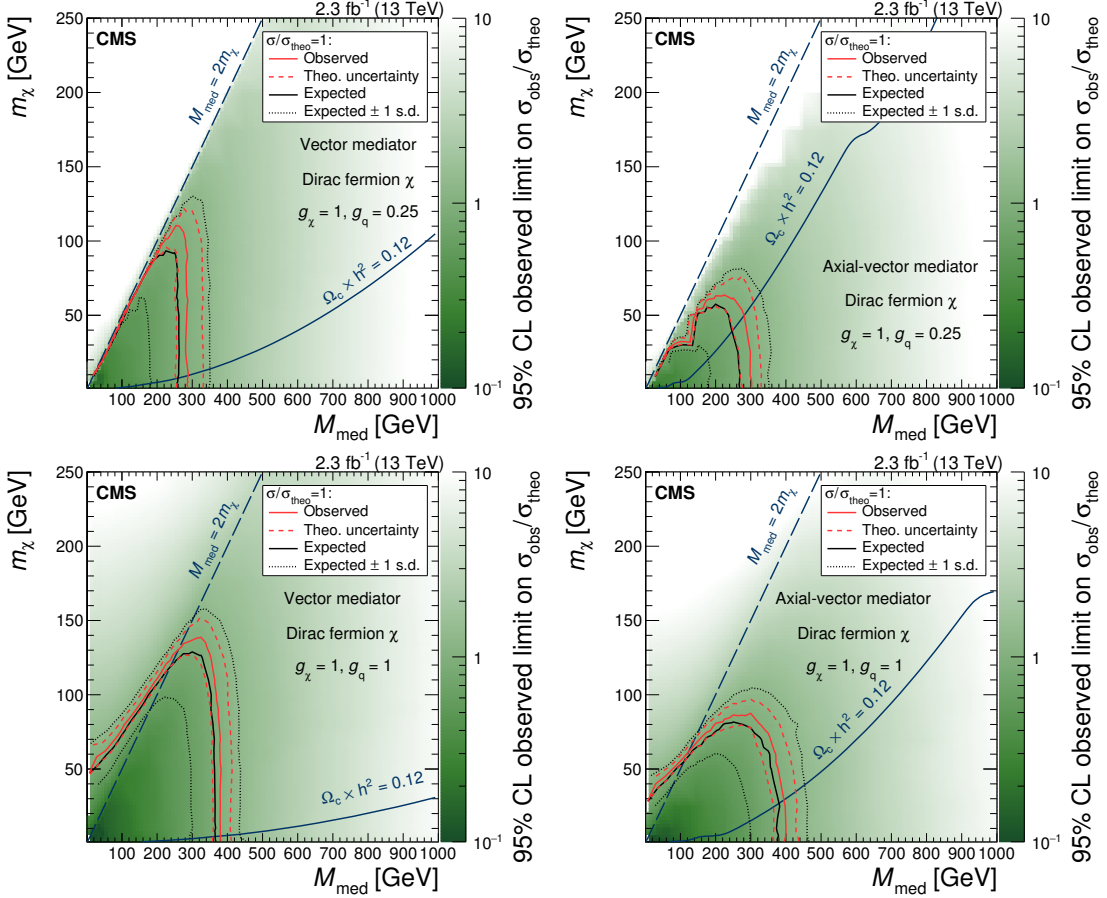


Figure 6. The 95% CL observed limits on the signal strength $\sigma_{\text{obs}}/\sigma_{\text{theo}}$ in both vector (left) and axial-vector (right) mediator scenarios, for mediator-quark coupling constant values $g_q = 0.25$ (upper) and 1 (lower). In all cases, the DM-mediator coupling g_χ is set to one. The expected exclusion curves for unity signal strength are shown as a reference, with black dashed lines indicating the expected ± 1 s.d. interval due to experimental uncertainties. The red dashed lines show the influence of theory-related signal normalization uncertainties on the observed limits, which are estimated to be 15%. The solid line labeled “ $\Omega_c \times h^2 = 0.12$ ” identifies the parameter region where no additional new physics beyond the simplified model is necessary to reproduce the observed DM relic abundance [1, 35, 72–74].

the efficiency of reconstructing potential signal events depends on the characteristics of the signal, the model-independent limits are not corrected for the efficiency. For the models considered in this analysis, typical efficiencies are in the range 50–70% (simplified DM model), 60–70% (EFT DM model), and 55–60% (unparticle model). The efficiencies are calculated as the ratio of the number of simulated events passing the final selection to the number of simulated events passing the selection criteria at the generator level (acceptance).

9 Summary

A search for physics beyond the standard model has been performed in events with a Z boson and missing transverse momentum, using a data set corresponding to an integrated luminosity of 2.3 fb^{-1} of pp collisions at a center-of-mass energy of 13 TeV. The observed

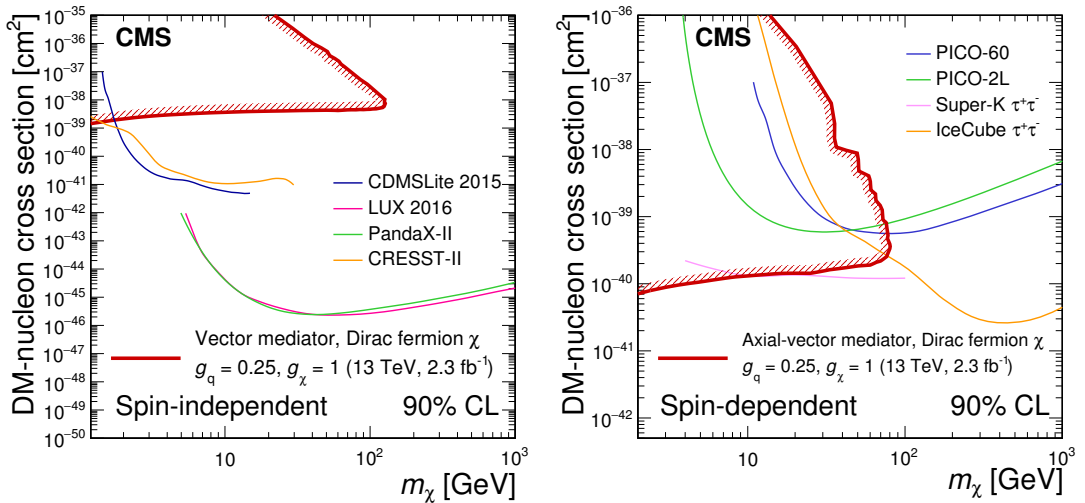


Figure 7. Observed 90% CL limits on the DM-nucleon scattering cross sections in both spin-independent (left) and spin-dependent (right) cases, assuming a mediator-quark coupling constant $g_q = 0.25$ and mediator-DM coupling constant $g_\chi = 1$. The line shading indicates the excluded region. Limits from the LUX [75], CDMSLite [76], PandaX-II [77], and CRESST-II [78] experiments are shown for the spin-independent case. Limits from the Super-Kamiokande [79], PICO-2L [80], PICO-60 [81], and IceCube [82] experiments are shown for the spin-dependent case.

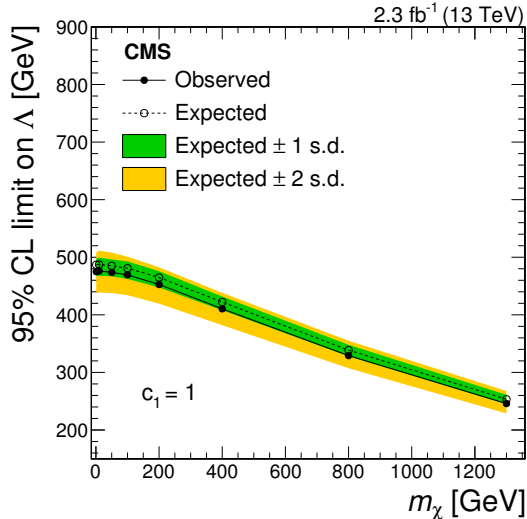


Figure 8. The 95% CL expected and observed limits on the cutoff scale Λ of the EFT benchmark of DM production as a function of DM particle mass m_χ .

data are consistent with the expected standard model processes. The results are analyzed to obtain limits in three different scenarios of physics beyond the standard model. In a simplified model of DM production via a vector or axial vector mediator, 95% confidence level limits are obtained on the masses of the DM particles and the mediator. Limits on the DM-nucleon scattering cross section are set at 90% confidence level in spin-dependent and spin-independent coupling scenarios. In an effective field theory approach, limits are set on the DM coupling parameters to U(1) and SU(2) gauge fields and on the scale of new

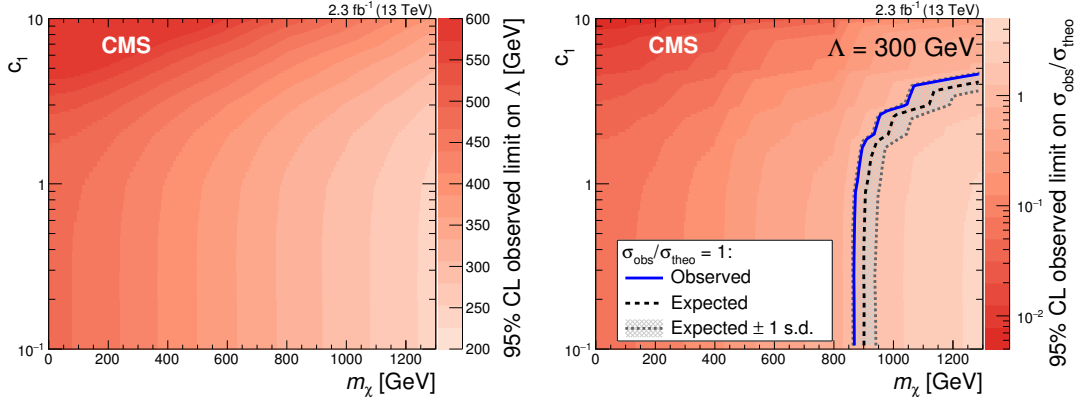


Figure 9. The 95% CL observed limits on the cutoff scale Λ (left) and signal strength $\sigma^{\text{obs}}/\sigma^{\text{th}}$ (right) as a function of coupling c_1 and DM mass m_χ . The expected exclusion curves for unit signal strength are shown as a reference. The gray shaded area bounded by gray dashed lines indicates the expected ± 1 s.d. interval due to experimental uncertainties.

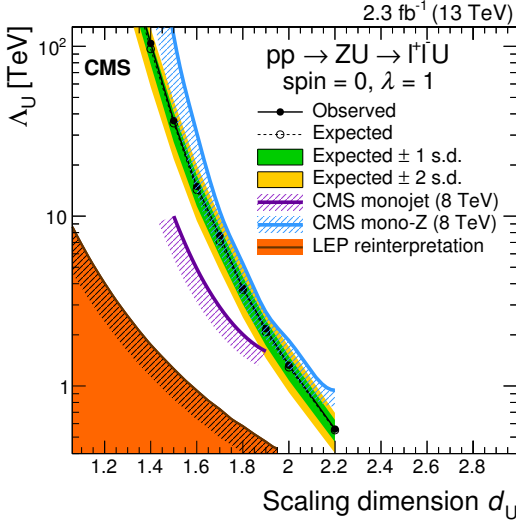


Figure 10. The 95% CL lower limits on unparticle effective cutoff scale Λ_U for a fixed coupling $\lambda = 1$. The results from CMS monojet [15] and mono-Z [17] searches, as well as a reinterpretation of LEP searches [83] are shown for comparison.

physics. For an unparticle model, 95% confidence level limits are obtained on the effective cutoff scale as a function of the scaling dimension. In addition, model-independent limits on the contribution to the visible $Z + E_T^{\text{miss}}$ cross section from non-standard-model sources are presented as a function of the minimum requirement on E_T^{miss} . These results are the first in this signal topology to be interpreted in terms of a simplified model. Furthermore, the limits on unparticle production are the first of their kind to be presented at $\sqrt{s} = 13$ TeV.

Acknowledgments

We congratulate our colleagues in the CERN accelerator departments for the excellent performance of the LHC and thank the technical and administrative staffs at CERN and

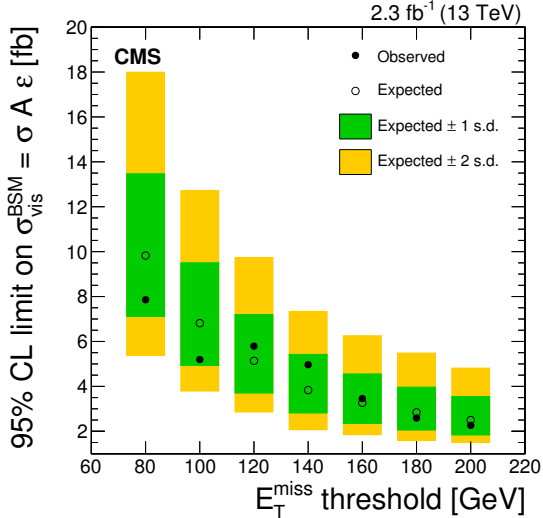


Figure 11. The model-independent upper limits at 95% CL on the visible cross section ($\sigma A \epsilon$) for BSM production of events, as a function of E_T^{miss} threshold. The values plotted correspond to those given in table 4.

E_T^{miss} threshold [GeV]	80	100	120	140	160	180	200
Total SM background	73.9	43.0	24.0	14.1	9.5	6.8	4.9
Total uncertainty	9.2	5.2	2.9	1.3	0.9	0.7	0.5
Data	66	37	26	17	10	6	4
Observed upper limit	18.1	11.9	13.3	11.4	8.0	6.0	5.2
Expected upper limit +2 s.d.	41.4	29.2	22.4	16.9	14.4	12.6	11.1
Expected upper limit +1 s.d.	31.0	21.9	16.5	12.5	10.5	9.1	8.1
Expected upper limit	22.6	15.7	11.8	8.8	7.5	6.5	5.8
Expected upper limit -1 s.d.	16.4	11.3	8.5	6.5	5.4	4.7	4.2
Expected upper limit -2 s.d.	12.4	8.7	6.6	4.8	4.3	3.7	3.5

Table 4. Total SM background predictions for the numbers of events passing the selection requirements, for different E_T^{miss} thresholds, compared with the observed numbers of events. The listed uncertainties include both statistical and systematic components. The 95% CL observed and expected upper limits for the contribution of events from BSM sources are also shown. In addition, the ± 1 s.d. and ± 2 s.d. excursions from expected limits are given.

at other CMS institutes for their contributions to the success of the CMS effort. In addition, we gratefully acknowledge the computing centres and personnel of the Worldwide LHC Computing Grid for delivering so effectively the computing infrastructure essential to our analyses. Finally, we acknowledge the enduring support for the construction and operation of the LHC and the CMS detector provided by the following funding agencies: BMWFW and FWF (Austria); FNRS and FWO (Belgium); CNPq, CAPES, FAPERJ, and FAPESP (Brazil); MES (Bulgaria); CERN; CAS, MoST, and NSFC (China); COLCIENCIAS (Colombia); MSES and CSF (Croatia); RPF (Cyprus); SENESCYT (Ecuador); MoER, ERC IUT and ERDF (Estonia); Academy of Finland, MEC, and HIP (Finland);

CEA and CNRS/IN2P3 (France); BMBF, DFG, and HGF (Germany); GSRT (Greece); OTKA and NIH (Hungary); DAE and DST (India); IPM (Iran); SFI (Ireland); INFN (Italy); MSIP and NRF (Republic of Korea); LAS (Lithuania); MOE and UM (Malaysia); BUAP, CINVESTAV, CONACYT, LNS, SEP, and UASLP-FAI (Mexico); MBIE (New Zealand); PAEC (Pakistan); MSHE and NSC (Poland); FCT (Portugal); JINR (Dubna); MON, RosAtom, RAS and RFBR (Russia); MESTD (Serbia); SEIDI and CPAN (Spain); Swiss Funding Agencies (Switzerland); MST (Taipei); ThEPCenter, IPST, STAR and NSTDA (Thailand); TUBITAK and TAEK (Turkey); NASU and SFFR (Ukraine); STFC (United Kingdom); DOE and NSF (U.S.A.).

Individuals have received support from the Marie-Curie programme and the European Research Council and EPLANET (European Union); the Leventis Foundation; the A. P. Sloan Foundation; the Alexander von Humboldt Foundation; the Belgian Federal Science Policy Office; the Fonds pour la Formation à la Recherche dans l’Industrie et dans l’Agriculture (FRIA-Belgium); the Agentschap voor Innovatie door Wetenschap en Technologie (IWT-Belgium); the Ministry of Education, Youth and Sports (MEYS) of the Czech Republic; the Council of Science and Industrial Research, India; the HOMING PLUS programme of the Foundation for Polish Science, cofinanced from European Union, Regional Development Fund, the Mobility Plus programme of the Ministry of Science and Higher Education, the National Science Center (Poland), contracts Harmonia 2014/14/M/ST2/00428, Opus 2013/11/B/ST2/04202, 2014/13/B/ST2/02543 and 2014/15/B/ST2/03998, Sonata-bis 2012/07/E/ST2/01406; the Thalis and Aristeia programmes cofinanced by EU-ESF and the Greek NSRF; the National Priorities Research Program by Qatar National Research Fund; the Programa Clarín-COFUND del Principado de Asturias; the Rachadapisek Sompot Fund for Postdoctoral Fellowship, Chulalongkorn University and the Chulalongkorn Academic into Its 2nd Century Project Advancement Project (Thailand); and the Welch Foundation, contract C-1845.

Open Access. This article is distributed under the terms of the Creative Commons Attribution License ([CC-BY 4.0](#)), which permits any use, distribution and reproduction in any medium, provided the original author(s) and source are credited.

References

- [1] PLANCK collaboration, P.A.R. Ade et al., *Planck 2015 results. XIII. Cosmological parameters*, *Astron. Astrophys.* **594** (2016) A13 [[arXiv:1502.01589](#)] [[INSPIRE](#)].
- [2] P. Cushman et al., *Working group report: WIMP dark matter direct detection*, [arXiv:1310.8327](#) [[INSPIRE](#)].
- [3] J. Buckley et al., *Working group report: WIMP dark matter indirect detection*, [arXiv:1310.7040](#) [[INSPIRE](#)].
- [4] D. Abercrombie et al., *Dark matter benchmark models for early LHC run-2 searches: report of the ATLAS/CMS dark matter forum*, [arXiv:1507.00966](#) [[INSPIRE](#)].
- [5] ATLAS collaboration, *Search for dark matter in events with a hadronically decaying W or Z boson and missing transverse momentum in pp collisions at $\sqrt{s} = 8$ TeV with the ATLAS detector*, *Phys. Rev. Lett.* **112** (2014) 041802 [[arXiv:1309.4017](#)] [[INSPIRE](#)].

- [6] ATLAS collaboration, *Search for dark matter in events with a Z boson and missing transverse momentum in pp collisions at $\sqrt{s} = 8$ TeV with the ATLAS detector*, *Phys. Rev. D* **90** (2014) 012004 [[arXiv:1404.0051](#)] [[INSPIRE](#)].
- [7] ATLAS collaboration, *Search for new particles in events with one lepton and missing transverse momentum in pp collisions at $\sqrt{s} = 8$ TeV with the ATLAS detector*, *JHEP* **09** (2014) 037 [[arXiv:1407.7494](#)] [[INSPIRE](#)].
- [8] CMS collaboration, *Search for physics beyond the standard model in final states with a lepton and missing transverse energy in proton-proton collisions at $\sqrt{s} = 8$ TeV*, *Phys. Rev. D* **91** (2015) 092005 [[arXiv:1408.2745](#)] [[INSPIRE](#)].
- [9] ATLAS collaboration, *Search for dark matter in events with heavy quarks and missing transverse momentum in pp collisions with the ATLAS detector*, *Eur. Phys. J. C* **75** (2015) 92 [[arXiv:1410.4031](#)] [[INSPIRE](#)].
- [10] ATLAS collaboration, *Search for new phenomena in events with a photon and missing transverse momentum in pp collisions at $\sqrt{s} = 8$ TeV with the ATLAS detector*, *Phys. Rev. D* **91** (2015) 012008 [*Erratum ibid. D* **92** (2015) 059903] [[arXiv:1411.1559](#)] [[INSPIRE](#)].
- [11] CMS collaboration, *Search for monotop signatures in proton-proton collisions at $\sqrt{s} = 8$ TeV*, *Phys. Rev. Lett.* **114** (2015) 101801 [[arXiv:1410.1149](#)] [[INSPIRE](#)].
- [12] ATLAS collaboration, *Search for invisible particles produced in association with single-top-quarks in proton-proton collisions at $\sqrt{s} = 8$ TeV with the ATLAS detector*, *Eur. Phys. J. C* **75** (2015) 79 [[arXiv:1410.5404](#)] [[INSPIRE](#)].
- [13] ATLAS collaboration, *Search for dark matter in events with missing transverse momentum and a Higgs boson decaying to two photons in pp collisions at $\sqrt{s} = 8$ TeV with the ATLAS detector*, *Phys. Rev. Lett.* **115** (2015) 131801 [[arXiv:1506.01081](#)] [[INSPIRE](#)].
- [14] CMS collaboration, *Search for the production of dark matter in association with top-quark pairs in the single-lepton final state in proton-proton collisions at $\sqrt{s} = 8$ TeV*, *JHEP* **06** (2015) 121 [[arXiv:1504.03198](#)] [[INSPIRE](#)].
- [15] CMS collaboration, *Search for dark matter, extra dimensions and unparticles in monojet events in proton-proton collisions at $\sqrt{s} = 8$ TeV*, *Eur. Phys. J. C* **75** (2015) 235 [[arXiv:1408.3583](#)] [[INSPIRE](#)].
- [16] ATLAS collaboration, *Search for new phenomena in final states with an energetic jet and large missing transverse momentum in pp collisions at $\sqrt{s} = 8$ TeV with the ATLAS detector*, *Eur. Phys. J. C* **75** (2015) 299 [[arXiv:1502.01518](#)] [[INSPIRE](#)].
- [17] CMS collaboration, *Search for dark matter and unparticles produced in association with a Z boson in proton-proton collisions at $\sqrt{s} = 8$ TeV*, *Phys. Rev. D* **93** (2016) 052011 [[arXiv:1511.09375](#)] [[INSPIRE](#)].
- [18] CMS collaboration, *Search for new phenomena in monophoton final states in proton-proton collisions at $\sqrt{s} = 8$ TeV*, *Phys. Lett. B* **755** (2016) 102 [[arXiv:1410.8812](#)] [[INSPIRE](#)].
- [19] CMS collaboration, *Search for dark matter in proton-proton collisions at 8 TeV with missing transverse momentum and vector boson tagged jets*, *JHEP* **12** (2016) 083 [[arXiv:1607.05764](#)] [[INSPIRE](#)].
- [20] ATLAS collaboration, *Search for dark matter produced in association with a hadronically decaying vector boson in pp collisions at $\sqrt{s} = 13$ TeV with the ATLAS detector*, *Phys. Lett. B* **763** (2016) 251 [[arXiv:1608.02372](#)] [[INSPIRE](#)].

- [21] H. Georgi, *Unparticle physics*, *Phys. Rev. Lett.* **98** (2007) 221601 [[hep-ph/0703260](#)] [[INSPIRE](#)].
- [22] H. Georgi, *Another odd thing about unparticle physics*, *Phys. Lett. B* **650** (2007) 275 [[arXiv:0704.2457](#)] [[INSPIRE](#)].
- [23] K. Cheung, W.-Y. Keung and T.-C. Yuan, *Collider signals of unparticle physics*, *Phys. Rev. Lett.* **99** (2007) 051803 [[arXiv:0704.2588](#)] [[INSPIRE](#)].
- [24] K. Cheung, W.-Y. Keung and T.-C. Yuan, *Collider phenomenology of unparticle physics*, *Phys. Rev. D* **76** (2007) 055003 [[arXiv:0706.3155](#)] [[INSPIRE](#)].
- [25] Z. Kang, *Upgrading sterile neutrino dark matter to FIMP using scale invariance*, *Eur. Phys. J. C* **75** (2015) 471 [[arXiv:1411.2773](#)] [[INSPIRE](#)].
- [26] M. Rinaldi, G. Cognola, L. Vanzo and S. Zerbini, *Inflation in scale-invariant theories of gravity*, *Phys. Rev. D* **91** (2015) 123527 [[arXiv:1410.0631](#)] [[INSPIRE](#)].
- [27] H. Cheng, *The possible existence of Weyl's vector meson*, *Phys. Rev. Lett.* **61** (1988) 2182 [[INSPIRE](#)].
- [28] T. Banks and A. Zaks, *On the phase structure of vector-like gauge theories with massless fermions*, *Nucl. Phys. B* **196** (1982) 189 [[INSPIRE](#)].
- [29] S. Ask, I.V. Akin, L. Benucci, A. De Roeck, M. Goebel and J. Haller, *Real emission and virtual exchange of gravitons and unparticles in PYTHIA8*, *Comput. Phys. Commun.* **181** (2010) 1593 [[arXiv:0912.4233](#)] [[INSPIRE](#)].
- [30] CMS collaboration, *The CMS experiment at the CERN LHC*, 2008 *JINST* **3** S08004 [[INSPIRE](#)].
- [31] J. Alwall et al., *The automated computation of tree-level and next-to-leading order differential cross sections and their matching to parton shower simulations*, *JHEP* **07** (2014) 079 [[arXiv:1405.0301](#)] [[INSPIRE](#)].
- [32] T. Sjöstrand, S. Mrenna and P.Z. Skands, *A brief introduction to PYTHIA 8.1*, *Comput. Phys. Commun.* **178** (2008) 852 [[arXiv:0710.3820](#)] [[INSPIRE](#)].
- [33] CMS collaboration, *Event generator tunes obtained from underlying event and multiparton scattering measurements*, *Eur. Phys. J. C* **76** (2016) 155 [[arXiv:1512.00815](#)] [[INSPIRE](#)].
- [34] P. Skands, S. Carrazza and J. Rojo, *Tuning PYTHIA 8.1: the Monash 2013 tune*, *Eur. Phys. J. C* **74** (2014) 3024 [[arXiv:1404.5630](#)] [[INSPIRE](#)].
- [35] G. Busoni et al., *Recommendations on presenting LHC searches for missing transverse energy signals using simplified s-channel models of dark matter*, [arXiv:1603.04156](#) [[INSPIRE](#)].
- [36] S. Ask, *Simulation of Z plus graviton/unparticle production at the LHC*, *Eur. Phys. J. C* **60** (2009) 509 [[arXiv:0809.4750](#)] [[INSPIRE](#)].
- [37] P. Nason, *A new method for combining NLO QCD with shower Monte Carlo algorithms*, *JHEP* **11** (2004) 040 [[hep-ph/0409146](#)] [[INSPIRE](#)].
- [38] S. Frixione, P. Nason and C. Oleari, *Matching NLO QCD computations with parton shower simulations: the POWHEG method*, *JHEP* **11** (2007) 070 [[arXiv:0709.2092](#)] [[INSPIRE](#)].
- [39] S. Alioli, P. Nason, C. Oleari and E. Re, *A general framework for implementing NLO calculations in shower Monte Carlo programs: the POWHEG BOX*, *JHEP* **06** (2010) 043 [[arXiv:1002.2581](#)] [[INSPIRE](#)].

- [40] E. Re, *Single-top Wt-channel production matched with parton showers using the POWHEG method*, *Eur. Phys. J. C* **71** (2011) 1547 [[arXiv:1009.2450](#)] [[INSPIRE](#)].
- [41] S. Alioli, S.-O. Moch and P. Uwer, *Hadronic top-quark pair-production with one jet and parton showering*, *JHEP* **01** (2012) 137 [[arXiv:1110.5251](#)] [[INSPIRE](#)].
- [42] J.M. Campbell and R.K. Ellis, *MCFM for the Tevatron and the LHC*, *Nucl. Phys. Proc. Suppl.* **205-206** (2010) 10 [[arXiv:1007.3492](#)] [[INSPIRE](#)].
- [43] R. Gavin, Y. Li, F. Petriello and S. Quackenbush, *FEWZ 2.0: a code for hadronic Z production at next-to-next-to-leading order*, *Comput. Phys. Commun.* **182** (2011) 2388 [[arXiv:1011.3540](#)] [[INSPIRE](#)].
- [44] Y. Li and F. Petriello, *Combining QCD and electroweak corrections to dilepton production in the framework of the FEWZ simulation code*, *Phys. Rev. D* **86** (2012) 094034 [[arXiv:1208.5967](#)] [[INSPIRE](#)].
- [45] NNPDF collaboration, R.D. Ball et al., *Parton distributions for the LHC Run II*, *JHEP* **04** (2015) 040 [[arXiv:1410.8849](#)] [[INSPIRE](#)].
- [46] GEANT4 collaboration, S. Agostinelli et al., *GEANT4: a simulation toolkit*, *Nucl. Instrum. Meth. A* **506** (2003) 250 [[INSPIRE](#)].
- [47] J. Allison et al., *Geant4 developments and applications*, *IEEE Trans. Nucl. Sci.* **53** (2006) 270 [[INSPIRE](#)].
- [48] CMS collaboration, *CMS tracking performance results from early LHC operation*, *Eur. Phys. J. C* **70** (2010) 1165 [[arXiv:1007.1988](#)] [[INSPIRE](#)].
- [49] CMS collaboration, *Particle-flow event reconstruction in CMS and performance for jets, taus and MET*, *CMS-PAS-PFT-09-001* (2009).
- [50] CMS collaboration, *Commissioning of the particle-flow event reconstruction with the first LHC collisions recorded in the CMS detector*, *CMS-PAS-PFT-10-001* (2010).
- [51] CMS collaboration, *Performance of electron reconstruction and selection with the CMS detector in proton-proton collisions at $\sqrt{s} = 8$ TeV*, *2015 JINST* **10** P06005 [[arXiv:1502.02701](#)] [[INSPIRE](#)].
- [52] CMS collaboration, *Performance of CMS muon reconstruction in pp collision events at $\sqrt{s} = 7$ TeV*, *2012 JINST* **7** P10002 [[arXiv:1206.4071](#)] [[INSPIRE](#)].
- [53] CMS collaboration, *Reconstruction and identification of τ lepton decays to hadrons and ν_τ at CMS*, *2016 JINST* **11** P01019 [[arXiv:1510.07488](#)] [[INSPIRE](#)].
- [54] M. Cacciari, G.P. Salam and G. Soyez, *The anti- k_t jet clustering algorithm*, *JHEP* **04** (2008) 063 [[arXiv:0802.1189](#)] [[INSPIRE](#)].
- [55] M. Cacciari, G.P. Salam and G. Soyez, *FastJet user manual*, *Eur. Phys. J. C* **72** (2012) 1896 [[arXiv:1111.6097](#)] [[INSPIRE](#)].
- [56] M. Cacciari and G.P. Salam, *Dispelling the N^3 myth for the k_t jet-finder*, *Phys. Lett. B* **641** (2006) 57 [[hep-ph/0512210](#)] [[INSPIRE](#)].
- [57] CMS collaboration, *Jet energy scale and resolution in the CMS experiment in pp collisions at 8 TeV*, *2017 JINST* **12** P02014 [[arXiv:1607.03663](#)] [[INSPIRE](#)].
- [58] PARTICLE DATA GROUP collaboration, K.A. Olive et al., *Review of particle physics*, *Chin. Phys. C* **38** (2014) 090001 [[INSPIRE](#)].

- [59] CMS collaboration, *Identification of b -quark jets with the CMS experiment*, **2013 JINST 8 P04013** [[arXiv:1211.4462](#)] [[INSPIRE](#)].
- [60] CMS collaboration, *Identification of b quark jets at the CMS experiment in the LHC Run 2*, **CMS-PAS-BTV-15-001** (2015).
- [61] M. Grazzini, S. Kallweit and D. Rathlev, *ZZ production at the LHC: fiducial cross sections and distributions in NNLO QCD*, **Phys. Lett. B 750** (2015) 407 [[arXiv:1507.06257](#)] [[INSPIRE](#)].
- [62] A. Bierweiler, T. Kasprzik and J.H. Kühn, *Vector-boson pair production at the LHC to $\mathcal{O}(\alpha^3)$ accuracy*, **JHEP 12** (2013) 071 [[arXiv:1305.5402](#)] [[INSPIRE](#)].
- [63] S. Gieseke, T. Kasprzik and J.H. Kühn, *Vector-boson pair production and electroweak corrections in HERWIG++*, **Eur. Phys. J. C 74** (2014) 2988 [[arXiv:1401.3964](#)] [[INSPIRE](#)].
- [64] J. Baglio, L.D. Ninh and M.M. Weber, *Massive gauge boson pair production at the LHC: a next-to-leading order story*, **Phys. Rev. D 88** (2013) 113005 [*Erratum ibid. D 94* (2016) 099902] [[arXiv:1307.4331](#)] [[INSPIRE](#)].
- [65] CMS collaboration, *Measurement of the inclusive W and Z production cross sections in pp collisions at $\sqrt{s} = 7$ TeV*, **JHEP 10** (2011) 132 [[arXiv:1107.4789](#)] [[INSPIRE](#)].
- [66] J. Butterworth et al., *PDF4LHC recommendations for LHC run II*, **J. Phys. G 43** (2016) 023001 [[arXiv:1510.03865](#)] [[INSPIRE](#)].
- [67] CMS collaboration, *CMS luminosity measurement for the 2015 data-taking period*, **CMS-PAS-LUM-15-001** (2015).
- [68] ATLAS collaboration, *Measurement of the inelastic proton-proton cross section at $\sqrt{s} = 13$ TeV with the ATLAS detector at the LHC*, **Phys. Rev. Lett. 117** (2016) 182002 [[arXiv:1606.02625](#)] [[INSPIRE](#)].
- [69] T. Junk, *Confidence level computation for combining searches with small statistics*, **Nucl. Instrum. Meth. A 434** (1999) 435 [[hep-ex/9902006](#)] [[INSPIRE](#)].
- [70] A.L. Read, *Presentation of search results: the $CL(s)$ technique*, **J. Phys. G 28** (2002) 2693 [[INSPIRE](#)].
- [71] ATLAS and CMS collaborations and The LHC Higgs Combination Group, *Procedure for the LHC Higgs boson search combination in Summer 2011*, **ATL-PHYS-PUB-2011-11** (2011).
- [72] T. du Pree, K. Hahn, P. Harris and C. Roskas, *Cosmological constraints on dark matter models for collider searches*, [arXiv:1603.08525](#) [[INSPIRE](#)].
- [73] M. Backovic, K. Kong and M. McCaskey, *MadDM v.1.0: computation of dark matter relic abundance using MadGraph5*, **Physics of the Dark Universe 5-6** (2014) 18 [[arXiv:1308.4955](#)] [[INSPIRE](#)].
- [74] WMAP collaboration, G. Hinshaw et al., *Nine-year Wilkinson Microwave Anisotropy Probe (WMAP) observations: cosmological parameter results*, **Astrophys. J. Suppl. 208** (2013) 19 [[arXiv:1212.5226](#)] [[INSPIRE](#)].
- [75] LUX collaboration, D.S. Akerib et al., *Results from a search for dark matter in the complete LUX exposure*, **Phys. Rev. Lett. 118** (2017) 021303 [[arXiv:1608.07648](#)] [[INSPIRE](#)].
- [76] SUPERCDMS collaboration, R. Agnese et al., *New results from the search for low-mass weakly interacting massive particles with the CDMS low ionization threshold experiment*, **Phys. Rev. Lett. 116** (2016) 071301 [[arXiv:1509.02448](#)] [[INSPIRE](#)].

- [77] PANDAX-II collaboration, A. Tan et al., *Dark matter results from first 98.7 days of data from the PandaX-II experiment*, *Phys. Rev. Lett.* **117** (2016) 121303 [[arXiv:1607.07400](#)] [[INSPIRE](#)].
- [78] CRESST collaboration, G. Angloher et al., *Results on light dark matter particles with a low-threshold CRESST-II detector*, *Eur. Phys. J. C* **76** (2016) 25 [[arXiv:1509.01515](#)] [[INSPIRE](#)].
- [79] SUPER-KAMIOKANDE collaboration, K. Choi et al., *Search for neutrinos from annihilation of captured low-mass dark matter particles in the Sun by Super-Kamiokande*, *Phys. Rev. Lett.* **114** (2015) 141301 [[arXiv:1503.04858](#)] [[INSPIRE](#)].
- [80] PICO collaboration, C. Amole et al., *Improved dark matter search results from PICO-2L Run 2*, *Phys. Rev. D* **93** (2016) 061101 [[arXiv:1601.03729](#)] [[INSPIRE](#)].
- [81] PICO collaboration, C. Amole et al., *Dark matter search results from the PICO-60 CF₃I bubble chamber*, *Phys. Rev. D* **93** (2016) 052014 [[arXiv:1510.07754](#)] [[INSPIRE](#)].
- [82] ICECUBE collaboration, M.G. Aartsen et al., *Improved limits on dark matter annihilation in the Sun with the 79-string IceCube detector and implications for supersymmetry*, *JCAP* **04** (2016) 022 [[arXiv:1601.00653](#)] [[INSPIRE](#)].
- [83] S. Kathrein, S. Knapen and M.J. Strassler, *Bounds from LEP on unparticle interactions with electroweak bosons*, *Phys. Rev. D* **84** (2011) 015010 [[arXiv:1012.3737](#)] [[INSPIRE](#)].

The CMS collaboration

Yerevan Physics Institute, Yerevan, Armenia

A.M. Sirunyan, A. Tumasyan

Institut für Hochenergiephysik, Wien, Austria

W. Adam, E. Asilar, T. Bergauer, J. Brandstetter, E. Brondolin, M. Dragicevic, J. Erö, M. Flechl, M. Friedl, R. Frühwirth¹, V.M. Ghete, C. Hartl, N. Hörmann, J. Hrubec, M. Jeitler¹, A. König, I. Krätschmer, D. Liko, T. Matsushita, I. Mikulec, D. Rabady, N. Rad, B. Rahbaran, H. Rohringer, J. Schieck¹, J. Strauss, W. Waltenberger, C.-E. Wulz¹

Institute for Nuclear Problems, Minsk, Belarus

V. Chekhovsky, O. Dvornikov, Y. Dydyshka, I. Emelianchik, A. Litomin, V. Makarenko, V. Mossolov, R. Stefanovitch, J. Suarez Gonzalez, V. Zy kunov

National Centre for Particle and High Energy Physics, Minsk, Belarus

N. Shumeiko

Universiteit Antwerpen, Antwerpen, Belgium

S. Alderweireldt, E.A. De Wolf, X. Janssen, J. Lauwers, M. Van De Klundert, H. Van Haevermaet, P. Van Mechelen, N. Van Remortel, A. Van Spilbeeck

Vrije Universiteit Brussel, Brussel, Belgium

S. Abu Zeid, F. Blekman, J. D'Hondt, N. Daci, I. De Bruyn, K. Deroover, S. Lowette, S. Moortgat, L. Moreels, A. Olbrechts, Q. Python, K. Skovpen, S. Tavernier, W. Van Doninck, P. Van Mulders, I. Van Parijs

Université Libre de Bruxelles, Bruxelles, Belgium

H. Brun, B. Clerbaux, G. De Lentdecker, H. Delannoy, G. Fasanella, L. Favart, R. Goldouzian, A. Grebenyuk, G. Karapostoli, T. Lenzi, A. Léonard, J. Luetic, T. Maerschalk, A. Marinov, A. Randle-conde, T. Seva, C. Vander Velde, P. Vanlaer, D. Vannerom, R. Yonamine, F. Zenoni, F. Zhang²

Ghent University, Ghent, Belgium

A. Cimmino, T. Cornelis, D. Dobur, A. Fagot, M. Gul, I. Khvastunov, D. Poyraz, S. Salva, R. Schöfbeck, M. Tytgat, W. Van Driessche, E. Yazgan, N. Zaganidis

Université Catholique de Louvain, Louvain-la-Neuve, Belgium

H. Bakhshiansohi, C. Beluffi³, O. Bondu, S. Brochet, G. Bruno, A. Caudron, S. De Visscher, C. Delaere, M. Delcourt, B. Francois, A. Giannanco, A. Jafari, M. Komm, G. Krintiras, V. Lemaitre, A. Magitteri, A. Mertens, M. Musich, C. Nuttens, K. Piotrkowski, L. Quertenmont, M. Selvaggi, M. Vidal Marono, S. Wertz

Université de Mons, Mons, Belgium

N. Belyi

Centro Brasileiro de Pesquisas Fisicas, Rio de Janeiro, Brazil

W.L. Aldá Júnior, F.L. Alves, G.A. Alves, L. Brito, C. Hensel, A. Moraes, M.E. Pol, P. Rebello Teles

Universidade do Estado do Rio de Janeiro, Rio de Janeiro, Brazil

E. Belchior Batista Das Chagas, W. Carvalho, J. Chinellato⁴, A. Custódio, E.M. Da Costa, G.G. Da Silveira⁵, D. De Jesus Damiao, C. De Oliveira Martins, S. Fonseca De Souza, L.M. Huertas Guativa, H. Malbouisson, D. Matos Figueiredo, C. Mora Herrera, L. Mundim, H. Nogima, W.L. Prado Da Silva, A. Santoro, A. Sznajder, E.J. Tonelli Manganote⁴, A. Vilela Pereira

Universidade Estadual Paulista ^a, Universidade Federal do ABC ^b, São Paulo, Brazil

S. Ahuja^a, C.A. Bernardes^a, S. Dogra^a, T.R. Fernandez Perez Tomei^a, E.M. Gregores^b, P.G. Mercadante^b, C.S. Moon^a, S.F. Novaes^a, Sandra S. Padula^a, D. Romero Abad^b, J.C. Ruiz Vargas^a

Institute for Nuclear Research and Nuclear Energy, Sofia, Bulgaria

A. Aleksandrov, R. Hadjiiska, P. Iaydjiev, M. Rodozov, S. Stoykova, G. Sultanov, M. Vutova

University of Sofia, Sofia, Bulgaria

A. Dimitrov, I. Glushkov, L. Litov, B. Pavlov, P. Petkov

Beihang University, Beijing, China

W. Fang⁶

Institute of High Energy Physics, Beijing, China

M. Ahmad, J.G. Bian, G.M. Chen, H.S. Chen, M. Chen, Y. Chen⁷, T. Cheng, C.H. Jiang, D. Leggat, Z. Liu, F. Romeo, M. Ruan, S.M. Shaheen, A. Spiezia, J. Tao, C. Wang, Z. Wang, H. Zhang, J. Zhao

State Key Laboratory of Nuclear Physics and Technology, Peking University, Beijing, China

Y. Ban, G. Chen, Q. Li, S. Liu, Y. Mao, S.J. Qian, D. Wang, Z. Xu

Universidad de Los Andes, Bogota, Colombia

C. Avila, A. Cabrera, L.F. Chaparro Sierra, C. Florez, J.P. Gomez, C.F. González Hernández, J.D. Ruiz Alvarez, J.C. Sanabria

University of Split, Faculty of Electrical Engineering, Mechanical Engineering and Naval Architecture, Split, Croatia

N. Godinovic, D. Lelas, I. Puljak, P.M. Ribeiro Cipriano, T. Sculac

University of Split, Faculty of Science, Split, Croatia

Z. Antunovic, M. Kovac

Institute Rudjer Boskovic, Zagreb, Croatia

V. Brigljevic, D. Ferencek, K. Kadija, B. Mesic, S. Micanovic, L. Sudic, T. Susa

University of Cyprus, Nicosia, Cyprus

A. Attikis, G. Mavromanolakis, J. Mousa, C. Nicolaou, F. Ptochos, P.A. Razis, H. Rykaczewski, D. Tsiakkouri

Charles University, Prague, Czech Republic

M. Finger⁸, M. Finger Jr.⁸

Universidad San Francisco de Quito, Quito, Ecuador

E. Carrera Jarrin

**Academy of Scientific Research and Technology of the Arab Republic of Egypt,
Egyptian Network of High Energy Physics, Cairo, Egypt**

A.A. Abdelalim^{9,10}, A. Mohamed¹⁰, A. Mohamed¹¹

National Institute of Chemical Physics and Biophysics, Tallinn, Estonia

M. Kadastik, L. Perrini, M. Raidal, A. Tiko, C. Veelken

Department of Physics, University of Helsinki, Helsinki, Finland

P. Eerola, J. Pekkanen, M. Voutilainen

Helsinki Institute of Physics, Helsinki, Finland

J. Härkönen, T. Järvinen, V. Karimäki, R. Kinnunen, T. Lampén, K. Lassila-Perini,
S. Lehti, T. Lindén, P. Luukka, J. Tuominiemi, E. Tuovinen, L. Wendland

Lappeenranta University of Technology, Lappeenranta, Finland

J. Talvitie, T. Tuuva

IRFU, CEA, Université Paris-Saclay, Gif-sur-Yvette, France

M. Besancon, F. Couderc, M. Dejardin, D. Denegri, B. Fabbro, J.L. Faure, C. Favaro,
F. Ferri, S. Ganjour, S. Ghosh, A. Givernaud, P. Gras, G. Hamel de Monchenault, P. Jarry,
I. Kucher, E. Locci, M. Machet, J. Malcles, J. Rander, A. Rosowsky, M. Titov, A. Zghiche

**Laboratoire Leprince-Ringuet, Ecole Polytechnique, IN2P3-CNRS, Palaiseau,
France**

A. Abdulsalam, I. Antropov, S. Baffioni, F. Beaudette, P. Busson, L. Cadamuro,
E. Chapon, C. Charlot, O. Davignon, R. Granier de Cassagnac, M. Jo, S. Lisniak, P. Miné,
M. Nguyen, C. Ochando, G. Ortona, P. Paganini, P. Pigard, S. Regnard, R. Salerno,
Y. Sirois, T. Strebler, Y. Yilmaz, A. Zabi

**Institut Pluridisciplinaire Hubert Curien (IPHC), Université de Strasbourg,
CNRS-IN2P3**

J.-L. Agram¹², J. Andrea, A. Aubin, D. Bloch, J.-M. Brom, M. Buttignol, E.C. Chabert,
N. Chanon, C. Collard, E. Conte¹², X. Coubez, J.-C. Fontaine¹², D. Gelé, U. Goerlach,
A.-C. Le Bihan, P. Van Hove

**Centre de Calcul de l’Institut National de Physique Nucléaire et de Physique
des Particules, CNRS/IN2P3, Villeurbanne, France**

S. Gadrat

**Université de Lyon, Université Claude Bernard Lyon 1, CNRS-IN2P3, Institut
de Physique Nucléaire de Lyon, Villeurbanne, France**

S. Beauceron, C. Bernet, G. Boudoul, C.A. Carrillo Montoya, R. Chierici, D. Contardo,
B. Courbon, P. Depasse, H. El Mamouni, J. Fan, J. Fay, S. Gascon, M. Gouzevitch,

G. Grenier, B. Ille, F. Lagarde, I.B. Laktineh, M. Lethuillier, L. Mirabito, A.L. Pequegnot, S. Perries, A. Popov¹³, D. Sabes, V. Sordini, M. Vander Donckt, P. Verdier, S. Viret

Georgian Technical University, Tbilisi, Georgia

T. Toriashvili¹⁴

Tbilisi State University, Tbilisi, Georgia

Z. Tsamalaidze⁸

RWTH Aachen University, I. Physikalisches Institut, Aachen, Germany

C. Autermann, S. Beranek, L. Feld, M.K. Kiesel, K. Klein, M. Lipinski, M. Preuten, C. Schomakers, J. Schulz, T. Verlage

RWTH Aachen University, III. Physikalisches Institut A, Aachen, Germany

A. Albert, M. Brodski, E. Dietz-Laursonn, D. Duchardt, M. Endres, M. Erdmann, S. Erdweg, T. Esch, R. Fischer, A. Güth, M. Hamer, T. Hebbeker, C. Heidemann, K. Hoepfner, S. Knutzen, M. Merschmeyer, A. Meyer, P. Millet, S. Mukherjee, M. Olszewski, K. Padeken, T. Pook, M. Radziej, H. Reithler, M. Rieger, F. Scheuch, L. Sonnenschein, D. Teyssier, S. Thüer

RWTH Aachen University, III. Physikalisches Institut B, Aachen, Germany

V. Cherepanov, G. Flügge, B. Kargoll, T. Kress, A. Künsken, J. Lingemann, T. Müller, A. Nehrkorn, A. Nowack, C. Pistone, O. Pooth, A. Stahl¹⁵

Deutsches Elektronen-Synchrotron, Hamburg, Germany

M. Aldaya Martin, T. Arndt, C. Asawatangtrakuldee, K. Beernaert, O. Behnke, U. Behrens, A.A. Bin Anuar, K. Borras¹⁶, A. Campbell, P. Connor, C. Contreras-Campana, F. Costanza, C. Diez Pardos, G. Dolinska, G. Eckerlin, D. Eckstein, T. Eichhorn, E. Eren, E. Gallo¹⁷, J. Garay Garcia, A. Geiser, A. Gitzko, J.M. Grados Luyando, A. Grohsjean, P. Gunnellini, A. Harb, J. Hauk, M. Hempel¹⁸, H. Jung, A. Kalogeropoulos, O. Karacheban¹⁸, M. Kasemann, J. Keaveney, C. Kleinwort, I. Korol, D. Krücker, W. Lange, A. Lelek, J. Leonard, K. Lipka, A. Lobanova, W. Lohmann¹⁸, R. Mankel, I.-A. Melzer-Pellmann, A.B. Meyer, G. Mittag, J. Mnich, A. Mußgiller, E. Ntomari, D. Pitzl, R. Placakyte, A. Raspereza, B. Roland, M.Ö. Sahin, P. Saxena, T. Schoerner-Sadenius, C. Seitz, S. Spannagel, N. Stefaniuk, G.P. Van Onsem, R. Walsh, C. Wissing

University of Hamburg, Hamburg, Germany

V. Blobel, M. Centis Vignali, A.R. Draeger, T. Dreyer, E. Garutti, D. Gonzalez, J. Haller, M. Hoffmann, A. Junkes, R. Klanner, R. Kogler, N. Kovalchuk, T. Lapsien, T. Lenz, I. Marchesini, D. Marconi, M. Meyer, M. Niedziela, D. Nowatschin, F. Pantaleo¹⁵, T. Peiffer, A. Perieanu, J. Poehlsen, C. Sander, C. Scharf, P. Schleper, A. Schmidt, S. Schumann, J. Schwandt, H. Stadie, G. Steinbrück, F.M. Stober, M. Stöver, H. Tholen, D. Troendle, E. Usai, L. Vanelderden, A. Vanhoefer, B. Vormwald

Institut für Experimentelle Kernphysik, Karlsruhe, Germany

M. Akbiyik, C. Barth, S. Baur, C. Baus, J. Berger, E. Butz, R. Caspart, T. Chwalek, F. Colombo, W. De Boer, A. Dierlamm, S. Fink, B. Freund, R. Friese, M. Giffels, A. Gilbert,

P. Goldenzweig, D. Haitz, F. Hartmann¹⁵, S.M. Heindl, U. Husemann, I. Katkov¹³, S. Kudella, H. Mildner, M.U. Mozer, Th. Müller, M. Plagge, G. Quast, K. Rabbertz, S. Röcker, F. Roscher, M. Schröder, I. Shvetsov, G. Sieber, H.J. Simonis, R. Ulrich, S. Wayand, M. Weber, T. Weiler, S. Williamson, C. Wöhrmann, R. Wolf

Institute of Nuclear and Particle Physics (INPP), NCSR Demokritos, Aghia Paraskevi, Greece

G. Anagnostou, G. Daskalakis, T. Geralis, V.A. Giakoumopoulou, A. Kyriakis, D. Loukas, I. Topsis-Giotis

National and Kapodistrian University of Athens, Athens, Greece

S. Kesisoglou, A. Panagiotou, N. Saoulidou, E. Tziaferi

University of Ioánnina, Ioánnina, Greece

I. Evangelou, G. Flouris, C. Foudas, P. Kokkas, N. Loukas, N. Manthos, I. Papadopoulos, E. Paradas

MTA-ELTE Lendület CMS Particle and Nuclear Physics Group, Eötvös Loránd University, Budapest, Hungary

N. Filipovic

Wigner Research Centre for Physics, Budapest, Hungary

G. Bencze, C. Hajdu, D. Horvath¹⁹, F. Sikler, V. Veszpremi, G. Vesztregombi²⁰, A.J. Zsigmond

Institute of Nuclear Research ATOMKI, Debrecen, Hungary

N. Beni, S. Czellar, J. Karancsi²¹, A. Makovec, J. Molnar, Z. Szillasi

Institute of Physics, University of Debrecen

M. Bartók²⁰, P. Raics, Z.L. Trocsanyi, B. Ujvari

National Institute of Science Education and Research, Bhubaneswar, India

S. Bahinipati, S. Choudhury²², P. Mal, K. Mandal, A. Nayak²³, D.K. Sahoo, N. Sahoo, S.K. Swain

Panjab University, Chandigarh, India

S. Bansal, S.B. Beri, V. Bhatnagar, R. Chawla, U.Bhawandeep, A.K. Kalsi, A. Kaur, M. Kaur, R. Kumar, P. Kumari, A. Mehta, M. Mittal, J.B. Singh, G. Walia

University of Delhi, Delhi, India

Ashok Kumar, A. Bhardwaj, B.C. Choudhary, R.B. Garg, S. Keshri, S. Malhotra, M. Naimuddin, N. Nishu, K. Ranjan, R. Sharma, V. Sharma

Saha Institute of Nuclear Physics, Kolkata, India

R. Bhattacharya, S. Bhattacharya, K. Chatterjee, S. Dey, S. Dutt, S. Dutta, S. Ghosh, N. Majumdar, A. Modak, K. Mondal, S. Mukhopadhyay, S. Nandan, A. Purohit, A. Roy, D. Roy, S. Roy Chowdhury, S. Sarkar, M. Sharan, S. Thakur

Indian Institute of Technology Madras, Madras, India

P.K. Behera

Bhabha Atomic Research Centre, Mumbai, India

R. Chudasama, D. Dutta, V. Jha, V. Kumar, A.K. Mohanty¹⁵, P.K. Netrakanti, L.M. Pant, P. Shukla, A. Topkar

Tata Institute of Fundamental Research-A, Mumbai, India

T. Aziz, S. Dugad, G. Kole, B. Mahakud, S. Mitra, G.B. Mohanty, B. Parida, N. Sur, B. Sutar

Tata Institute of Fundamental Research-B, Mumbai, India

S. Banerjee, S. Bhowmik²⁴, R.K. Dewanjee, S. Ganguly, M. Guchait, Sa. Jain, S. Kumar, M. Maity²⁴, G. Majumder, K. Mazumdar, T. Sarkar²⁴, N. Wickramage²⁵

Indian Institute of Science Education and Research (IISER), Pune, India

S. Chauhan, S. Dube, V. Hegde, A. Kapoor, K. Kotheendar, S. Pandey, A. Rane, S. Sharma

Institute for Research in Fundamental Sciences (IPM), Tehran, Iran

S. Chenarani²⁶, E. Eskandari Tadavani, S.M. Etesami²⁶, M. Khakzad, M. Mohammadi Najafabadi, M. Naseri, S. Pakhtinat Mehdiabadi²⁷, F. Rezaei Hosseiniabadi, B. Safarzadeh²⁸, M. Zeinali

University College Dublin, Dublin, Ireland

M. Felcini, M. Grunewald

INFN Sezione di Bari ^a, Università di Bari ^b, Politecnico di Bari ^c, Bari, Italy

M. Abbrescia^{a,b}, C. Calabria^{a,b}, C. Caputo^{a,b}, A. Colaleo^a, D. Creanza^{a,c}, L. Cristella^{a,b}, N. De Filippis^{a,c}, M. De Palma^{a,b}, L. Fiore^a, G. Iaselli^{a,c}, G. Maggi^{a,c}, M. Maggi^a, G. Miniello^{a,b}, S. My^{a,b}, S. Nuzzo^{a,b}, A. Pompili^{a,b}, G. Pugliese^{a,c}, R. Radogna^{a,b}, A. Ranieri^a, G. Selvaggi^{a,b}, A. Sharma^a, L. Silvestris^{a,15}, R. Venditti^{a,b}, P. Verwilligen^a

INFN Sezione di Bologna ^a, Università di Bologna ^b, Bologna, Italy

G. Abbiendi^a, C. Battilana, D. Bonacorsi^{a,b}, S. Braibant-Giacomelli^{a,b}, L. Brigliadori^{a,b}, R. Campanini^{a,b}, P. Capiluppi^{a,b}, A. Castro^{a,b}, F.R. Cavallo^a, S.S. Chhibra^{a,b}, G. Codispoti^{a,b}, M. Cuffiani^{a,b}, G.M. Dallavalle^a, F. Fabbri^a, A. Fanfani^{a,b}, D. Fasanella^{a,b}, P. Giacomelli^a, C. Grandi^a, L. Guiducci^{a,b}, S. Marcellini^a, G. Masetti^a, A. Montanari^a, F.L. Navarria^{a,b}, A. Perrotta^a, A.M. Rossi^{a,b}, T. Rovelli^{a,b}, G.P. Siroli^{a,b}, N. Tosi^{a,b,15}

INFN Sezione di Catania ^a, Università di Catania ^b, Catania, Italy

S. Albergo^{a,b}, S. Costa^{a,b}, A. Di Mattia^a, F. Giordano^{a,b}, R. Potenza^{a,b}, A. Tricomi^{a,b}, C. Tuve^{a,b}

INFN Sezione di Firenze ^a, Università di Firenze ^b, Firenze, Italy

G. Barbagli^a, V. Ciulli^{a,b}, C. Civinini^a, R. D'Alessandro^{a,b}, E. Focardi^{a,b}, P. Lenzi^{a,b}, M. Meschini^a, S. Paoletti^a, G. Sguazzoni^a, L. Viliani^{a,b,15}

INFN Laboratori Nazionali di Frascati, Frascati, Italy

L. Benussi, S. Bianco, F. Fabbri, D. Piccolo, F. Primavera¹⁵

INFN Sezione di Genova ^a, Università di Genova ^b, Genova, Italy

V. Calvelli^{a,b}, F. Ferro^a, M.R. Monge^{a,b}, E. Robutti^a, S. Tosi^{a,b}

INFN Sezione di Milano-Bicocca ^a, Università di Milano-Bicocca ^b, Milano, Italy

L. Brianza^{a,b,15}, F. Brivio^{a,b}, V. Ciriolo, M.E. Dinardo^{a,b}, S. Fiorendi^{a,b,15}, S. Gennai^a, A. Ghezzi^{a,b}, P. Govoni^{a,b}, M. Malberti^{a,b}, S. Malvezzi^a, R.A. Manzoni^{a,b}, D. Menasce^a, L. Moroni^a, M. Paganoni^{a,b}, D. Pedrini^a, S. Pigazzini^{a,b}, S. Ragazzi^{a,b}, T. Tabarelli de Fatis^{a,b}

INFN Sezione di Napoli ^a, Università di Napoli 'Federico II' ^b, Napoli, Italy, Università della Basilicata ^c, Potenza, Italy, Università G. Marconi ^d, Roma, Italy

S. Buontempo^a, N. Cavallo^{a,c}, G. De Nardo, S. Di Guida^{a,d,15}, M. Esposito^{a,b}, F. Fabozzi^{a,c}, F. Fienga^{a,b}, A.O.M. Iorio^{a,b}, G. Lanza^a, L. Lista^a, S. Meola^{a,d,15}, P. Paolucci^{a,15}, C. Sciacca^{a,b}, F. Thyssen^a

INFN Sezione di Padova ^a, Università di Padova ^b, Padova, Italy, Università di Trento ^c, Trento, Italy

P. Azzi^{a,15}, N. Bacchetta^a, L. Benato^{a,b}, D. Bisello^{a,b}, A. Boletti^{a,b}, R. Carlin^{a,b}, P. Checchia^a, M. Dall'Osso^{a,b}, P. De Castro Manzano^a, T. Dorigo^a, U. Gasparini^{a,b}, A. Gozzelino^a, M. Gulmini^{a,29}, S. Lacaprara^a, M. Margoni^{a,b}, G. Maron^{a,29}, A.T. Meneguzzo^{a,b}, J. Pazzini^{a,b}, N. Pozzobon^{a,b}, P. Ronchese^{a,b}, F. Simonetto^{a,b}, E. Torassa^a, S. Ventura^a, M. Zanetti^{a,b}, P. Zotto^{a,b}, G. Zumerle^{a,b}

INFN Sezione di Pavia ^a, Università di Pavia ^b, Pavia, Italy

A. Braghieri^a, F. Fallavollita^{a,b}, A. Magnani^{a,b}, P. Montagna^{a,b}, S.P. Ratti^{a,b}, V. Re^a, C. Riccardi^{a,b}, P. Salvini^a, I. Vai^{a,b}, P. Vitulo^{a,b}

INFN Sezione di Perugia ^a, Università di Perugia ^b, Perugia, Italy

L. Alunni Solestizi^{a,b}, G.M. Bilei^a, D. Ciangottini^{a,b}, L. Fanò^{a,b}, P. Lariccia^{a,b}, R. Leonardi^{a,b}, G. Mantovani^{a,b}, M. Menichelli^a, A. Saha^a, A. Santocchia^{a,b}

INFN Sezione di Pisa ^a, Università di Pisa ^b, Scuola Normale Superiore di Pisa ^c, Pisa, Italy

K. Androssov^{a,30}, P. Azzurri^{a,15}, G. Bagliesi^a, J. Bernardini^a, T. Boccali^a, R. Castaldi^a, M.A. Ciocci^{a,30}, R. Dell'Orso^a, S. Donato^{a,c}, G. Fedi, A. Giassi^a, M.T. Grippo^{a,30}, F. Ligabue^{a,c}, T. Lomtadze^a, L. Martini^{a,b}, A. Messineo^{a,b}, F. Palla^a, A. Rizzi^{a,b}, A. Savoy-Navarro^{a,31}, P. Spagnolo^a, R. Tenchini^a, G. Tonelli^{a,b}, A. Venturi^a, P.G. Verdini^a

INFN Sezione di Roma ^a, Università di Roma ^b, Roma, Italy

L. Barone^{a,b}, F. Cavallari^a, M. Cipriani^{a,b}, D. Del Re^{a,b,15}, M. Diemoz^a, S. Gelli^{a,b}, E. Longo^{a,b}, F. Margaroli^{a,b}, B. Marzocchi^{a,b}, P. Meridiani^a, G. Organtini^{a,b}, R. Paramatti^a, F. Preiato^{a,b}, S. Rahatlou^{a,b}, C. Rovelli^a, F. Santanastasio^{a,b}

INFN Sezione di Torino ^a, Università di Torino ^b, Torino, Italy, Università del Piemonte Orientale ^c, Novara, Italy

N. Amapane^{a,b}, R. Arcidiacono^{a,c,15}, S. Argiro^{a,b}, M. Arneodo^{a,c}, N. Bartosik^a, R. Bellan^{a,b}, C. Biino^a, N. Cartiglia^a, F. Cenna^{a,b}, M. Costa^{a,b}, R. Covarelli^{a,b}, A. Degano^{a,b}, N. Demaria^a, L. Finco^{a,b}, B. Kiani^{a,b}, C. Mariotti^a, S. Maselli^a,

E. Migliore^{a,b}, V. Monaco^{a,b}, E. Monteil^{a,b}, M. Monteno^a, M.M. Obertino^{a,b}, L. Pacher^{a,b}, N. Pastrone^a, M. Pelliccioni^a, G.L. Pinna Angioni^{a,b}, F. Ravera^{a,b}, A. Romero^{a,b}, M. Ruspa^{a,c}, R. Sacchi^{a,b}, K. Shchelina^{a,b}, V. Sola^a, A. Solano^{a,b}, A. Staiano^a, P. Traczyk^{a,b}

INFN Sezione di Trieste ^a, Università di Trieste ^b, Trieste, Italy

S. Belforte^a, M. Casarsa^a, F. Cossutti^a, G. Della Ricca^{a,b}, A. Zanetti^a

Kyungpook National University, Daegu, Korea

D.H. Kim, G.N. Kim, M.S. Kim, S. Lee, S.W. Lee, Y.D. Oh, S. Sekmen, D.C. Son, Y.C. Yang

Chonbuk National University, Jeonju, Korea

A. Lee

Chonnam National University, Institute for Universe and Elementary Particles, Kwangju, Korea

H. Kim

Hanyang University, Seoul, Korea

J.A. Brochero Cifuentes, T.J. Kim

Korea University, Seoul, Korea

S. Cho, S. Choi, Y. Go, D. Gyun, S. Ha, B. Hong, Y. Jo, Y. Kim, K. Lee, K.S. Lee, S. Lee, J. Lim, S.K. Park, Y. Roh

Seoul National University, Seoul, Korea

J. Almond, J. Kim, H. Lee, S.B. Oh, B.C. Radburn-Smith, S.h. Seo, U.K. Yang, H.D. Yoo, G.B. Yu

University of Seoul, Seoul, Korea

M. Choi, H. Kim, J.H. Kim, J.S.H. Lee, I.C. Park, G. Ryu, M.S. Ryu

Sungkyunkwan University, Suwon, Korea

Y. Choi, J. Goh, C. Hwang, J. Lee, I. Yu

Vilnius University, Vilnius, Lithuania

V. Dudenas, A. Juodagalvis, J. Vaitkus

National Centre for Particle Physics, Universiti Malaya, Kuala Lumpur, Malaysia

I. Ahmed, Z.A. Ibrahim, J.R. Komaragiri, M.A.B. Md Ali³², F. Mohamad Idris³³, W.A.T. Wan Abdullah, M.N. Yusli, Z. Zolkapli

Centro de Investigacion y de Estudios Avanzados del IPN, Mexico City, Mexico

H. Castilla-Valdez, E. De La Cruz-Burelo, I. Heredia-De La Cruz³⁴, A. Hernandez-Almada, R. Lopez-Fernandez, R. Magaña Villalba, J. Mejia Guisao, A. Sanchez-Hernandez

Universidad Iberoamericana, Mexico City, Mexico

S. Carrillo Moreno, C. Oropeza Barrera, F. Vazquez Valencia

Benemerita Universidad Autonoma de Puebla, Puebla, Mexico

S. Carpinteyro, I. Pedraza, H.A. Salazar Ibarguen, C. Uribe Estrada

Universidad Autónoma de San Luis Potosí, San Luis Potosí, Mexico

A. Morelos Pineda

University of Auckland, Auckland, New Zealand

D. Kroccheck

University of Canterbury, Christchurch, New Zealand

P.H. Butler

National Centre for Physics, Quaid-I-Azam University, Islamabad, Pakistan

A. Ahmad, M. Ahmad, Q. Hassan, H.R. Hoorani, W.A. Khan, A. Saddique, M.A. Shah, M. Shoaib, M. Waqas

National Centre for Nuclear Research, Swierk, Poland

H. Bialkowska, M. Bluj, B. Boimska, T. Frueboes, M. Górska, M. Kazana, K. Nawrocki, K. Romanowska-Rybinska, M. Szleper, P. Zalewski

Institute of Experimental Physics, Faculty of Physics, University of Warsaw, Warsaw, PolandK. Bunkowski, A. Byszuk³⁵, K. Doroba, A. Kalinowski, M. Konecki, J. Krolikowski, M. Misiura, M. Olszewski, M. Walczak**Laboratório de Instrumentação e Física Experimental de Partículas, Lisboa, Portugal**

P. Bargassa, C. Beirão Da Cruz E Silva, B. Calpas, A. Di Francesco, P. Faccioli, P.G. Ferreira Parracho, M. Gallinaro, J. Hollar, N. Leonardo, L. Lloret Iglesias, M.V. Nemallapudi, J. Rodrigues Antunes, J. Seixas, O. Toldaiev, D. Vadruccio, J. Varela, P. Vischia

Joint Institute for Nuclear Research, Dubna, RussiaS. Afanasiev, V. Alexakhin, P. Bunin, M. Gavrilenko, I. Golutvin, I. Gorbunov, V. Karjavin, A. Lanev, A. Malakhov, V. Matveev^{36,37}, V. Palichik, V. Perelygin, M. Savina, S. Shmatov, N. Skatchkov, V. Smirnov, N. Voytishin, A. Zarubin**Petersburg Nuclear Physics Institute, Gatchina (St. Petersburg), Russia**L. Chtchipounov, V. Golovtsov, Y. Ivanov, V. Kim³⁸, E. Kuznetsova³⁹, V. Murzin, V. Oreshkin, V. Sulimov, A. Vorobyev**Institute for Nuclear Research, Moscow, Russia**

Yu. Andreev, A. Dermenev, S. Gninenko, N. Golubev, A. Karneyeu, M. Kirsanov, N. Krasnikov, A. Pashenkov, D. Tlisov, A. Toropin

Institute for Theoretical and Experimental Physics, Moscow, Russia

V. Epshteyn, V. Gavrilov, N. Lychkovskaya, V. Popov, I. Pozdnyakov, G. Safronov, A. Spiridonov, M. Toms, E. Vlasov, A. Zhokin

Moscow Institute of Physics and Technology, Moscow, RussiaA. Bylinkin³⁷

National Research Nuclear University 'Moscow Engineering Physics Institute' (MEPhI), Moscow, Russia

M. Chadeeva⁴⁰, O. Markin, V. Rusinov

P.N. Lebedev Physical Institute, Moscow, Russia

V. Andreev, M. Azarkin³⁷, I. Dremin³⁷, M. Kirakosyan, A. Leonidov³⁷, A. Terkulov

Skobeltsyn Institute of Nuclear Physics, Lomonosov Moscow State University, Moscow, Russia

A. Baskakov, A. Belyaev, E. Boos, M. Dubinin⁴¹, L. Dudko, A. Ershov, A. Gribushin, V. Klyukhin, O. Kodolova, I. Lokhtin, I. Miagkov, S. Obraztsov, S. Petrushanko, V. Savrin, A. Snigirev

Novosibirsk State University (NSU), Novosibirsk, Russia

V. Blinov⁴², Y. Skovpen⁴², D. Shtol⁴²

State Research Center of Russian Federation, Institute for High Energy Physics, Protvino, Russia

I. Azhgirey, I. Bayshev, S. Bitioukov, D. Elumakhov, V. Kachanov, A. Kalinin, D. Konstantinov, V. Krychkine, V. Petrov, R. Ryutin, A. Sobol, S. Troshin, N. Tyurin, A. Uzunian, A. Volkov

University of Belgrade, Faculty of Physics and Vinca Institute of Nuclear Sciences, Belgrade, Serbia

P. Adzic⁴³, P. Cirkovic, D. Devetak, M. Dordevic, J. Milosevic, V. Rekovic

Centro de Investigaciones Energéticas Medioambientales y Tecnológicas (CIEMAT), Madrid, Spain

J. Alcaraz Maestre, M. Barrio Luna, E. Calvo, M. Cerrada, M. Chamizo Llatas, N. Collino, B. De La Cruz, A. Delgado Peris, A. Escalante Del Valle, C. Fernandez Bedoya, J.P. Fernandez Ramos, J. Flix, M.C. Fouz, P. Garcia-Abia, O. Gonzalez Lopez, S. Goy Lopez, J.M. Hernandez, M.I. Josa, E. Navarro De Martino, A. Perez-Calero Yzquierdo, J. Puerta Pelayo, A. Quintario Olmeda, I. Redondo, L. Romero, M.S. Soares

Universidad Autónoma de Madrid, Madrid, Spain

J.F. de Trocóniz, M. Missiroli, D. Moran

Universidad de Oviedo, Oviedo, Spain

J. Cuevas, J. Fernandez Menendez, I. Gonzalez Caballero, J.R. González Fernández, E. Palencia Cortezon, S. Sanchez Cruz, I. Suárez Andrés, J.M. Vizan Garcia

Instituto de Física de Cantabria (IFCA), CSIC-Universidad de Cantabria, Santander, Spain

I.J. Cabrillo, A. Calderon, J.R. Castiñeiras De Saa, E. Curras, M. Fernandez, J. Garcia-Ferrero, G. Gomez, A. Lopez Virto, J. Marco, C. Martinez Rivero, F. Matorras, J. Piedra Gomez, T. Rodrigo, A. Ruiz-Jimeno, L. Scodellaro, N. Trevisani, I. Vila, R. Vilar Cortabitarte

CERN, European Organization for Nuclear Research, Geneva, Switzerland

D. Abbaneo, E. Auffray, G. Auzinger, M. Bachtis, P. Baillon, A.H. Ball, D. Barney, P. Bloch, A. Bocci, A. Bonato, C. Botta, T. Camporesi, R. Castello, M. Cepeda, G. Cerminara, Y. Chen, D. d'Enterria, A. Dabrowski, V. Daponte, A. David, M. De Gruttola, A. De Roeck, E. Di Marco⁴⁴, M. Dobson, B. Dorney, T. du Pree, D. Duggan, M. Dünser, N. Dupont, A. Elliott-Peisert, P. Everaerts, S. Fartoukh, G. Franzoni, J. Fulcher, W. Funk, D. Gigi, K. Gill, M. Girone, F. Glege, D. Gulhan, S. Gundacker, M. Guthoff, J. Hammer, P. Harris, J. Hegeman, V. Innocente, P. Janot, J. Kieseler, H. Kirschenmann, V. Knünz, A. Kornmayer¹⁵, M.J. Kortelainen, K. Kousouris, M. Krammer¹, C. Lange, P. Lecoq, C. Lourenço, M.T. Lucchini, L. Malgeri, M. Mannelli, A. Martelli, F. Meijers, J.A. Merlin, S. Mersi, E. Meschi, P. Milenovic⁴⁵, F. Moortgat, S. Morovic, M. Mulders, H. Neugebauer, S. Orfanelli, L. Orsini, L. Pape, E. Perez, M. Peruzzi, A. Petrilli, G. Petrucciani, A. Pfeiffer, M. Pierini, A. Racz, T. Reis, G. Rolandi⁴⁶, M. Rovere, H. Sakulin, J.B. Sauvan, C. Schäfer, C. Schwick, M. Seidel, A. Sharma, P. Silva, P. Sphicas⁴⁷, J. Steggemann, M. Stoye, Y. Takahashi, M. Tosi, D. Treille, A. Triossi, A. Tsirou, V. Veckalns⁴⁸, G.I. Veres²⁰, M. Verweij, N. Wardle, H.K. Wöhri, A. Zagozdzinska³⁵, W.D. Zeuner

Paul Scherrer Institut, Villigen, Switzerland

W. Bertl, K. Deiters, W. Erdmann, R. Horisberger, Q. Ingram, H.C. Kaestli, D. Kotlinski, U. Langenegger, T. Rohe

Institute for Particle Physics, ETH Zurich, Zurich, Switzerland

F. Bachmair, L. Bäni, L. Bianchini, B. Casal, G. Dissertori, M. Dittmar, M. Donegà, C. Grab, C. Heidegger, D. Hits, J. Hoss, G. Kasieczka, P. Lecomte[†], W. Lustermann, B. Mangano, M. Marionneau, P. Martinez Ruiz del Arbol, M. Masciovecchio, M.T. Meinhard, D. Meister, F. Micheli, P. Musella, F. Nessi-Tedaldi, F. Pandolfi, J. Pata, F. Pauss, G. Perrin, L. Perrozzi, M. Quittnat, M. Rossini, M. Schönenberger, A. Starodumov⁴⁹, V.R. Tavolaro, K. Theofilatos, R. Wallny

Universität Zürich, Zurich, Switzerland

T.K. Arrestad, C. Amsler⁵⁰, L. Caminada, M.F. Canelli, A. De Cosa, C. Galloni, A. Hinzmann, T. Hreus, B. Kilminster, J. Ngadiuba, D. Pinna, G. Rauco, P. Robmann, D. Salerno, Y. Yang, A. Zucchetta

National Central University, Chung-Li, Taiwan

V. Candelise, T.H. Doan, Sh. Jain, R. Khurana, M. Konyushikhin, C.M. Kuo, W. Lin, Y.J. Lu, A. Pozdnyakov, S.S. Yu

National Taiwan University (NTU), Taipei, Taiwan

Arun Kumar, P. Chang, Y.H. Chang, Y. Chao, K.F. Chen, P.H. Chen, F. Fiori, W.-S. Hou, Y. Hsiung, Y.F. Liu, R.-S. Lu, M. Miñano Moya, E. Paganis, A. Psallidas, J.f. Tsai

Chulalongkorn University, Faculty of Science, Department of Physics, Bangkok, Thailand

B. Asavapibhop, G. Singh, N. Srimanobhas, N. Suwonjandee

Cukurova University - Physics Department, Science and Art Faculty

A. Adiguzel, M.N. Bakirci⁵¹, S. Cerci⁵², S. Damarseckin, Z.S. Demiroglu, C. Dozen, I. Dumanoglu, S. Girgis, G. Gokbulut, Y. Guler, I. Hos⁵³, E.E. Kangal⁵⁴, O. Kara, A. Kayis Topaksu, U. Kiminsu, M. Oglakci, G. Onengut⁵⁵, K. Ozdemir⁵⁶, B. Tali⁵², S. Turkcapar, I.S. Zorbakir, C. Zorbilmez

Middle East Technical University, Physics Department, Ankara, Turkey

B. Bilin, S. Bilmis, B. Isildak⁵⁷, G. Karapinar⁵⁸, M. Yalvac, M. Zeyrek

Bogazici University, Istanbul, Turkey

E. Glmez, M. Kaya⁵⁹, O. Kaya⁶⁰, E.A. Yetkin⁶¹, T. Yetkin⁶²

Istanbul Technical University, Istanbul, Turkey

A. Cakir, K. Cankocak, S. Sen⁶³

Institute for Scintillation Materials of National Academy of Science of Ukraine, Kharkov, Ukraine

B. Grynyov

National Scientific Center, Kharkov Institute of Physics and Technology, Kharkov, Ukraine

L. Levchuk, P. Sorokin

University of Bristol, Bristol, United Kingdom

R. Aggleton, F. Ball, L. Beck, J.J. Brooke, D. Burns, E. Clement, D. Cussans, H. Flacher, J. Goldstein, M. Grimes, G.P. Heath, H.F. Heath, J. Jacob, L. Kreczko, C. Lucas, D.M. Newbold⁶⁴, S. Paramesvaran, A. Poll, T. Sakuma, S. Seif El Nasr-storey, D. Smith, V.J. Smith

Rutherford Appleton Laboratory, Didcot, United Kingdom

K.W. Bell, A. Belyaev⁶⁵, C. Brew, R.M. Brown, L. Calligaris, D. Cieri, D.J.A. Cockerill, J.A. Coughlan, K. Harder, S. Harper, E. Olaiya, D. Petyt, C.H. Shepherd-Themistocleous, A. Thea, I.R. Tomalin, T. Williams

Imperial College, London, United Kingdom

M. Baber, R. Bainbridge, O. Buchmuller, A. Bundock, D. Burton, S. Casasso, M. Citron, D. Colling, L. Corpe, P. Dauncey, G. Davies, A. De Wit, M. Della Negra, R. Di Maria, P. Dunne, A. Elwood, D. Futyana, Y. Haddad, G. Hall, G. Iles, T. James, R. Lane, C. Laner, R. Lucas⁶⁴, L. Lyons, A.-M. Magnan, S. Malik, L. Mastrolorenzo, J. Nash, A. Nikitenko⁴⁹, J. Pela, B. Penning, M. Pesaresi, D.M. Raymond, A. Richards, A. Rose, C. Seez, S. Summers, A. Tapper, K. Uchida, M. Vazquez Acosta⁶⁶, T. Virdee¹⁵, J. Wright, S.C. Zenz

Brunel University, Uxbridge, United Kingdom

J.E. Cole, P.R. Hobson, A. Khan, P. Kyberd, D. Leslie, I.D. Reid, P. Symonds, L. Teodorescu, M. Turner

Baylor University, Waco, U.S.A.

A. Borzou, K. Call, J. Dittmann, K. Hatakeyama, H. Liu, N. Pastika

The University of Alabama, Tuscaloosa, U.S.A.

S.I. Cooper, C. Henderson, P. Rumerio, C. West

Boston University, Boston, U.S.A.

D. Arcaro, A. Avetisyan, T. Bose, D. Gastler, D. Rankin, C. Richardson, J. Rohlf, L. Sulak, D. Zou

Brown University, Providence, U.S.A.

G. Benelli, D. Cutts, A. Garabedian, J. Hakala, U. Heintz, J.M. Hogan, O. Jesus, K.H.M. Kwok, E. Laird, G. Landsberg, Z. Mao, M. Narain, S. Piperov, S. Sagir, E. Spencer, R. Syarif

University of California, Davis, Davis, U.S.A.

R. Breedon, D. Burns, M. Calderon De La Barca Sanchez, S. Chauhan, M. Chertok, J. Conway, R. Conway, P.T. Cox, R. Erbacher, C. Flores, G. Funk, M. Gardner, W. Ko, R. Lander, C. Mclean, M. Mulhearn, D. Pellett, J. Pilot, S. Shalhout, J. Smith, M. Squires, D. Stolp, M. Tripathi

University of California, Los Angeles, U.S.A.

C. Bravo, R. Cousins, A. Dasgupta, A. Florent, J. Hauser, M. Ignatenko, N. Mccoll, D. Saltzberg, C. Schnaible, V. Valuev, M. Weber

University of California, Riverside, Riverside, U.S.A.

E. Bouvier, K. Burt, R. Clare, J. Ellison, J.W. Gary, S.M.A. Ghiasi Shirazi, G. Hansson, J. Heilman, P. Jandir, E. Kennedy, F. Lacroix, O.R. Long, M. Olmedo Negrete, M.I. Paneva, A. Shrinivas, W. Si, H. Wei, S. Wimpenny, B. R. Yates

University of California, San Diego, La Jolla, U.S.A.

J.G. Branson, G.B. Cerati, S. Cittolin, M. Derdzinski, R. Gerosa, A. Holzner, D. Klein, V. Krutelyov, J. Letts, I. Macneill, D. Olivito, S. Padhi, M. Pieri, M. Sani, V. Sharma, S. Simon, M. Tadel, A. Vartak, S. Wasserbaech⁶⁷, C. Welke, J. Wood, F. Würthwein, A. Yagil, G. Zevi Della Porta

University of California, Santa Barbara - Department of Physics, Santa Barbara, U.S.A.

N. Amin, R. Bhandari, J. Bradmiller-Feld, C. Campagnari, A. Dishaw, V. Dutta, M. Franco Sevilla, C. George, F. Golf, L. Gouskos, J. Gran, R. Heller, J. Incandela, S.D. Mullin, A. Ovcharova, H. Qu, J. Richman, D. Stuart, I. Suarez, J. Yoo

California Institute of Technology, Pasadena, U.S.A.

D. Anderson, J. Bendavid, A. Bornheim, J. Bunn, J. Duarte, J.M. Lawhorn, A. Mott, H.B. Newman, C. Pena, M. Spiropulu, J.R. Vlimant, S. Xie, R.Y. Zhu

Carnegie Mellon University, Pittsburgh, U.S.A.

M.B. Andrews, T. Ferguson, M. Paulini, J. Russ, M. Sun, H. Vogel, I. Vorobiev, M. Weinberg

University of Colorado Boulder, Boulder, U.S.A.

J.P. Cumalat, W.T. Ford, F. Jensen, A. Johnson, M. Krohn, T. Mulholland, K. Stenson, S.R. Wagner

Cornell University, Ithaca, U.S.A.

J. Alexander, J. Chaves, J. Chu, S. Dittmer, K. Mcdermott, N. Mirman, G. Nicolas Kaufman, J.R. Patterson, A. Rinkevicius, A. Ryd, L. Skinnari, L. Soffi, S.M. Tan, Z. Tao, J. Thom, J. Tucker, P. Wittich, M. Zientek

Fairfield University, Fairfield, U.S.A.

D. Winn

Fermi National Accelerator Laboratory, Batavia, U.S.A.

S. Abdullin, M. Albrow, G. Apollinari, A. Apresyan, S. Banerjee, L.A.T. Bauerdi^ck, A. Beretvas, J. Berryhill, P.C. Bhat, G. Bolla, K. Burkett, J.N. Butler, H.W.K. Cheung, F. Chlebana, S. Cihangir[†], M. Cremonesi, V.D. Elvira, I. Fisk, J. Freeman, E. Gottschalk, L. Gray, D. Green, S. Grünendahl, O. Gutsche, D. Hare, R.M. Harris, S. Hasegawa, J. Hirschauer, Z. Hu, B. Jayatilaka, S. Jindariani, M. Johnson, U. Joshi, B. Klima, B. Kreis, S. Lammel, J. Linacre, D. Lincoln, R. Lipton, M. Liu, T. Liu, R. Lopes De Sá, J. Lykken, K. Maeshima, N. Magini, J.M. Marraffino, S. Maruyama, D. Mason, P. McBride, P. Merkel, S. Mrenna, S. Nahm, V. O'Dell, K. Pedro, O. Prokofyev, G. Rakness, L. Ristori, E. Sexton-Kennedy, A. Soha, W.J. Spalding, L. Spiegel, S. Stoynev, J. Strait, N. Strobbe, L. Taylor, S. Tkaczyk, N.V. Tran, L. Uplegger, E.W. Vaandering, C. Vernieri, M. Verzocchi, R. Vidal, M. Wang, H.A. Weber, A. Whitbeck, Y. Wu

University of Florida, Gainesville, U.S.A.

D. Acosta, P. Avery, P. Bortignon, D. Bourilkov, A. Brinkerhoff, A. Carnes, M. Carver, D. Curry, S. Das, R.D. Field, I.K. Furic, J. Konigsberg, A. Korytov, J.F. Low, P. Ma, K. Matchev, H. Mei, G. Mitselmakher, D. Rank, L. Shchutska, D. Sperka, L. Thomas, J. Wang, S. Wang, J. Yelton

Florida International University, Miami, U.S.A.

S. Linn, P. Markowitz, G. Martinez, J.L. Rodriguez

Florida State University, Tallahassee, U.S.A.

A. Ackert, T. Adams, A. Askew, S. Bein, S. Hagopian, V. Hagopian, K.F. Johnson, H. Prosper, A. Santra, R. Yohay

Florida Institute of Technology, Melbourne, U.S.A.

M.M. Baarmand, V. Bhopatkar, S. Colafranceschi, M. Hohlmann, D. Noonan, T. Roy, F. Yumiceva

University of Illinois at Chicago (UIC), Chicago, U.S.A.

M.R. Adams, L. Apanasevich, D. Berry, R.R. Betts, I. Bucinskaite, R. Cavanaugh, O. Evdokimov, L. Gauthier, C.E. Gerber, D.J. Hofman, K. Jung, I.D. Sandoval Gonzalez, N. Varelas, H. Wang, Z. Wu, M. Zakaria, J. Zhang

The University of Iowa, Iowa City, U.S.A.

B. Bilki⁶⁸, W. Clarida, K. Dilsiz, S. Durgut, R.P. Gandrajula, M. Haytmyradov, V. Khristenko, J.-P. Merlo, H. Mermerkaya⁶⁹, A. Mestvirishvili, A. Moeller, J. Nachtman, H. Ogul, Y. Onel, F. Ozok⁷⁰, A. Penzo, C. Snyder, E. Tiras, J. Wetzel, K. Yi

Johns Hopkins University, Baltimore, U.S.A.

I. Anderson, B. Blumenfeld, A. Cocoros, N. Eminizer, D. Fehling, L. Feng, A.V. Gritsan, P. Maksimovic, C. Martin, M. Osherson, J. Roskes, U. Sarica, M. Swartz, M. Xiao, Y. Xin, C. You

The University of Kansas, Lawrence, U.S.A.

A. Al-bataineh, P. Baringer, A. Bean, S. Boren, J. Bowen, J. Castle, L. Forthomme, R.P. Kenny III, S. Khalil, A. Kropivnitskaya, D. Majumder, W. Mcbrayer, M. Murray, S. Sanders, R. Stringer, J.D. Tapia Takaki, Q. Wang

Kansas State University, Manhattan, U.S.A.

A. Ivanov, K. Kaadze, Y. Maravin, A. Mohammadi, L.K. Saini, N. Skhirtladze, S. Toda

Lawrence Livermore National Laboratory, Livermore, U.S.A.

F. Rebassoo, D. Wright

University of Maryland, College Park, U.S.A.

C. Anelli, A. Baden, O. Baron, A. Belloni, B. Calvert, S.C. Eno, C. Ferraioli, J.A. Gomez, N.J. Hadley, S. Jabeen, R.G. Kellogg, T. Kolberg, J. Kunkle, Y. Lu, A.C. Mignerey, F. Ricci-Tam, Y.H. Shin, A. Skuja, M.B. Tonjes, S.C. Tonwar

Massachusetts Institute of Technology, Cambridge, U.S.A.

D. Abercrombie, B. Allen, A. Apyan, V. Azzolini, R. Barbieri, A. Baty, R. Bi, K. Bierwagen, S. Brandt, W. Busza, I.A. Cali, M. D'Alfonso, Z. Demiragli, L. Di Matteo, G. Gomez Ceballos, M. Goncharov, D. Hsu, Y. Iiyama, G.M. Innocenti, M. Klute, D. Kovalevskyi, K. Krajcziar, Y.S. Lai, Y.-J. Lee, A. Levin, P.D. Luckey, B. Maier, A.C. Marini, C. McGinn, C. Mironov, S. Narayanan, X. Niu, C. Paus, C. Roland, G. Roland, J. Salfeld-Nebgen, G.S.F. Stephans, K. Tatar, M. Varma, D. Velicanu, J. Veverka, J. Wang, T.W. Wang, B. Wyslouch, M. Yang

University of Minnesota, Minneapolis, U.S.A.

A.C. Benvenuti, R.M. Chatterjee, A. Evans, P. Hansen, S. Kalafut, S.C. Kao, Y. Kubota, Z. Lesko, J. Mans, S. Nourbakhsh, N. Ruckstuhl, R. Rusack, N. Tambe, J. Turkewitz

University of Mississippi, Oxford, U.S.A.

J.G. Acosta, S. Oliveros

University of Nebraska-Lincoln, Lincoln, U.S.A.

E. Avdeeva, R. Bartek⁷¹, K. Bloom, D.R. Claes, A. Dominguez⁷¹, C. Fangmeier, R. Gonzalez Suarez, R. Kamalieddin, I. Kravchenko, A. Malta Rodrigues, F. Meier, J. Monroy, J.E. Siado, G.R. Snow, B. Stieger

State University of New York at Buffalo, Buffalo, U.S.A.

M. Alyari, J. Dolen, A. Godshalk, C. Harrington, I. Iashvili, J. Kaisen, A. Kharchilava, A. Parker, S. Rappoccio, B. Roozbahani

Northeastern University, Boston, U.S.A.

G. Alverson, E. Barberis, A. Hortiangtham, A. Massironi, D.M. Morse, D. Nash, T. Ori-moto, R. Teixeira De Lima, D. Trocino, R.-J. Wang, D. Wood

Northwestern University, Evanston, U.S.A.

S. Bhattacharya, O. Charaf, K.A. Hahn, A. Kumar, N. Mucia, N. Odell, B. Pollack, M.H. Schmitt, K. Sung, M. Trovato, M. Velasco

University of Notre Dame, Notre Dame, U.S.A.

N. Dev, M. Hildreth, K. Hurtado Anampa, C. Jessop, D.J. Karmgard, N. Kellams, K. Lannon, N. Marinelli, F. Meng, C. Mueller, Y. Musienko³⁶, M. Planer, A. Reinsvold, R. Ruchti, G. Smith, S. Taroni, M. Wayne, M. Wolf, A. Woodard

The Ohio State University, Columbus, U.S.A.

J. Alimena, L. Antonelli, B. Bylsma, L.S. Durkin, S. Flowers, B. Francis, A. Hart, C. Hill, R. Hughes, W. Ji, B. Liu, W. Luo, D. Puigh, B.L. Winer, H.W. Wulsin

Princeton University, Princeton, U.S.A.

S. Cooperstein, O. Driga, P. Elmer, J. Hardenbrook, P. Hebda, D. Lange, J. Luo, D. Mar-low, T. Medvedeva, K. Mei, J. Olsen, C. Palmer, P. Piroué, D. Stickland, A. Svyatkovskiy, C. Tully

University of Puerto Rico, Mayaguez, U.S.A.

S. Malik

Purdue University, West Lafayette, U.S.A.

A. Barker, V.E. Barnes, S. Folgueras, L. Gutay, M.K. Jha, M. Jones, A.W. Jung, A. Khatiwada, D.H. Miller, N. Neumeister, J.F. Schulte, X. Shi, J. Sun, F. Wang, W. Xie

Purdue University Calumet, Hammond, U.S.A.

N. Parashar, J. Stupak

Rice University, Houston, U.S.A.

A. Adair, B. Akgun, Z. Chen, K.M. Ecklund, F.J.M. Geurts, M. Guilbaud, W. Li, B. Michlin, M. Northup, B.P. Padley, J. Roberts, J. Rorie, Z. Tu, J. Zabel

University of Rochester, Rochester, U.S.A.

B. Betchart, A. Bodek, P. de Barbaro, R. Demina, Y.t. Duh, T. Ferbel, M. Galanti, A. Garcia-Bellido, J. Han, O. Hindrichs, A. Khukhunaishvili, K.H. Lo, P. Tan, M. Verzetti

Rutgers, The State University of New Jersey, Piscataway, U.S.A.

A. Agapitos, J.P. Chou, Y. Gershtein, T.A. Gómez Espinosa, E. Halkiadakis, M. Heindl, E. Hughes, S. Kaplan, R. Kunnnawalkam Elayavalli, S. Kyriacou, A. Lath, K. Nash, H. Saka, S. Salur, S. Schnetzer, D. Sheffield, S. Somalwar, R. Stone, S. Thomas, P. Thomassen, M. Walker

University of Tennessee, Knoxville, U.S.A.

A.G. Delannoy, M. Foerster, J. Heideman, G. Riley, K. Rose, S. Spanier, K. Thapa

Texas A&M University, College Station, U.S.A.

O. Bouhalil⁷², A. Celik, M. Dalchenko, M. De Mattia, A. Delgado, S. Dildick, R. Eusebi, J. Gilmore, T. Huang, E. Juska, T. Kamon⁷³, R. Mueller, Y. Pakhotin, R. Patel, A. Perloff, L. Perniè, D. Rathjens, A. Safonov, A. Tatarinov, K.A. Ulmer

Texas Tech University, Lubbock, U.S.A.

N. Akchurin, C. Cowden, J. Damgov, F. De Guio, C. Dragoiu, P.R. Dudero, J. Faulkner, E. Gurpinar, S. Kunori, K. Lamichhane, S.W. Lee, T. Libeiro, T. Peltola, S. Undleeb, I. Volobouev, Z. Wang

Vanderbilt University, Nashville, U.S.A.

S. Greene, A. Gurrola, R. Janjam, W. Johns, C. Maguire, A. Melo, H. Ni, P. Sheldon, S. Tuo, J. Velkovska, Q. Xu

University of Virginia, Charlottesville, U.S.A.

M.W. Arenton, P. Barria, B. Cox, J. Goodell, R. Hirosky, A. Ledovskoy, H. Li, C. Neu, T. Sinhuprasith, X. Sun, Y. Wang, E. Wolfe, F. Xia

Wayne State University, Detroit, U.S.A.

C. Clarke, R. Harr, P.E. Karchin, J. Sturdy

University of Wisconsin - Madison, Madison, WI, U.S.A.

D.A. Belknap, J. Buchanan, C. Caillol, S. Dasu, L. Dodd, S. Duric, B. Gomber, M. Grothe, M. Herndon, A. Hervé, P. Klabbers, A. Lanaro, A. Levine, K. Long, R. Loveless, I. Ojalvo, T. Perry, G.A. Pierro, G. Polese, T. Ruggles, A. Savin, N. Smith, W.H. Smith, D. Taylor, N. Woods

†: Deceased

- 1: Also at Vienna University of Technology, Vienna, Austria
- 2: Also at State Key Laboratory of Nuclear Physics and Technology, Peking University, Beijing, China
- 3: Also at Institut Pluridisciplinaire Hubert Curien (IPHC), Université de Strasbourg, CNRS/IN2P3, Strasbourg, France
- 4: Also at Universidade Estadual de Campinas, Campinas, Brazil
- 5: Also at Universidade Federal de Pelotas, Pelotas, Brazil
- 6: Also at Université Libre de Bruxelles, Bruxelles, Belgium
- 7: Also at Deutsches Elektronen-Synchrotron, Hamburg, Germany
- 8: Also at Joint Institute for Nuclear Research, Dubna, Russia
- 9: Also at Helwan University, Cairo, Egypt
- 10: Now at Zewail City of Science and Technology, Zewail, Egypt
- 11: Also at Ain Shams University, Cairo, Egypt
- 12: Also at Université de Haute Alsace, Mulhouse, France
- 13: Also at Skobeltsyn Institute of Nuclear Physics, Lomonosov Moscow State University, Moscow, Russia
- 14: Also at Tbilisi State University, Tbilisi, Georgia

- 15: Also at CERN, European Organization for Nuclear Research, Geneva, Switzerland
- 16: Also at RWTH Aachen University, III. Physikalisches Institut A, Aachen, Germany
- 17: Also at University of Hamburg, Hamburg, Germany
- 18: Also at Brandenburg University of Technology, Cottbus, Germany
- 19: Also at Institute of Nuclear Research ATOMKI, Debrecen, Hungary
- 20: Also at MTA-ELTE Lendület CMS Particle and Nuclear Physics Group, Eötvös Loránd University, Budapest, Hungary
- 21: Also at Institute of Physics, University of Debrecen, Debrecen, Hungary
- 22: Also at Indian Institute of Science Education and Research, Bhopal, India
- 23: Also at Institute of Physics, Bhubaneswar, India
- 24: Also at University of Visva-Bharati, Santiniketan, India
- 25: Also at University of Ruhuna, Matara, Sri Lanka
- 26: Also at Isfahan University of Technology, Isfahan, Iran
- 27: Also at Yazd University, Yazd, Iran
- 28: Also at Plasma Physics Research Center, Science and Research Branch, Islamic Azad University, Tehran, Iran
- 29: Also at Laboratori Nazionali di Legnaro dell'INFN, Legnaro, Italy
- 30: Also at Università degli Studi di Siena, Siena, Italy
- 31: Also at Purdue University, West Lafayette, U.S.A.
- 32: Also at International Islamic University of Malaysia, Kuala Lumpur, Malaysia
- 33: Also at Malaysian Nuclear Agency, MOSTI, Kajang, Malaysia
- 34: Also at Consejo Nacional de Ciencia y Tecnología, Mexico city, Mexico
- 35: Also at Warsaw University of Technology, Institute of Electronic Systems, Warsaw, Poland
- 36: Also at Institute for Nuclear Research, Moscow, Russia
- 37: Now at National Research Nuclear University 'Moscow Engineering Physics Institute' (MEPhI), Moscow, Russia
- 38: Also at St. Petersburg State Polytechnical University, St. Petersburg, Russia
- 39: Also at University of Florida, Gainesville, U.S.A.
- 40: Also at P.N. Lebedev Physical Institute, Moscow, Russia
- 41: Also at California Institute of Technology, Pasadena, U.S.A.
- 42: Also at Budker Institute of Nuclear Physics, Novosibirsk, Russia
- 43: Also at Faculty of Physics, University of Belgrade, Belgrade, Serbia
- 44: Also at INFN Sezione di Roma; Università di Roma, Roma, Italy
- 45: Also at University of Belgrade, Faculty of Physics and Vinca Institute of Nuclear Sciences, Belgrade, Serbia
- 46: Also at Scuola Normale e Sezione dell'INFN, Pisa, Italy
- 47: Also at National and Kapodistrian University of Athens, Athens, Greece
- 48: Also at Riga Technical University, Riga, Latvia
- 49: Also at Institute for Theoretical and Experimental Physics, Moscow, Russia
- 50: Also at Albert Einstein Center for Fundamental Physics, Bern, Switzerland
- 51: Also at Gaziosmanpasa University, Tokat, Turkey
- 52: Also at Adiyaman University, Adiyaman, Turkey
- 53: Also at Istanbul Aydin University, Istanbul, Turkey
- 54: Also at Mersin University, Mersin, Turkey
- 55: Also at Cag University, Mersin, Turkey
- 56: Also at Piri Reis University, Istanbul, Turkey
- 57: Also at Ozyegin University, Istanbul, Turkey
- 58: Also at Izmir Institute of Technology, Izmir, Turkey

- 59: Also at Marmara University, Istanbul, Turkey
- 60: Also at Kafkas University, Kars, Turkey
- 61: Also at Istanbul Bilgi University, Istanbul, Turkey
- 62: Also at Yildiz Technical University, Istanbul, Turkey
- 63: Also at Hacettepe University, Ankara, Turkey
- 64: Also at Rutherford Appleton Laboratory, Didcot, United Kingdom
- 65: Also at School of Physics and Astronomy, University of Southampton, Southampton, United Kingdom
- 66: Also at Instituto de Astrofísica de Canarias, La Laguna, Spain
- 67: Also at Utah Valley University, Orem, U.S.A.
- 68: Also at Argonne National Laboratory, Argonne, U.S.A.
- 69: Also at Erzincan University, Erzincan, Turkey
- 70: Also at Mimar Sinan University, Istanbul, Istanbul, Turkey
- 71: Now at The Catholic University of America, Washington, U.S.A.
- 72: Also at Texas A&M University at Qatar, Doha, Qatar
- 73: Also at Kyungpook National University, Daegu, Korea